Journal of Organometallic Chemistry 694 (2009) 1509–1523

Contents lists available at ScienceDirect

Journal of Organometallic Chemistry

journal homepage: www.elsevier.com/locate/jorganchem

Synthesis, structures and full characterization of *p-tert*-butylcalix[5]arene mono-, di-, tri- and pentaanionic ligand precursors

Daniel Mendoza-Espinosa [a], Bernat A. Martinez-Ortega [a], Mauricio Quiroz-Guzman [a], James A. Golen [b], Arnold L. Rheingold [b], Tracy A. Hanna [a,*]

[a] Department of Chemistry, Texas Christian University, Box 298860, Fort Worth, TX 76129, United States
[b] Department of Chemistry and Biochemistry, University of California, San Diego, 9500 Gilman Drive, m/c 0358, La Jolla, CA 92093-0358, United States

ARTICLE INFO

Article history:
Received 8 December 2008
Received in revised form 22 December 2008
Accepted 23 December 2008
Available online 8 January 2009

Keywords:
Calixarene
Alkali metal salts
Metal-arene π interactions
Conformations

ABSTRACT

The synthesis, complete characterization, and solid state conformation of a new series of *p-tert*-butylcalix[5]arene (**Bu^{t}C5**) mono-, di-, tri- and pentaanions are reported. X-ray structures of the alkali metal salts illustrate the strong influence of the alkali metal ion on the structure of the calixanion. The strength of the alkali metal base and its reaction stoichiometry play an important role in the conformation and level of deprotonation of the resulting anion. Reaction of **Bu^{t}C5** in a 2:1 molar ratio with alkali metal bases M_2CO_3 (M = Rb, Cs), or in a 1:1 ratio with M_2CO_3 (M = Na, K), MOH (M = Na, K, Rb, Cs) or MH (M = Li, Na) produces **Bu^{t}C5** monoanions, but **Bu^{t}C5** reacts in a 1:1 molar ratio with M_2CO_3 (M = Rb, Cs) or a 1:2 molar ratio with $MOC(CH_3)_3$ (M = Na, K) to afford **Bu^{t}C5** dianions. Due to the steric bulkiness of the Bu^t group no polymeric structures are observed. Alkali metal salts of trianionic **Bu^{t}C5** were obtained in high yields from reactions of **Bu^{t}C5** with $MOC(CH_3)_3$ (M = Li, Na, K), Bu^{n}Li, LiH and LiOH in a 1:3 molar ratio. Pentaanionic **Bu^{t}C5** salts were obtained by the reaction with $MOC(CH_3)_3$ (M = Li, Na, K) or Bu^{n}Li in a 5:1 ratio. X-ray crystal structures of **Bu^{t}C5** · Na and **Bu^{t}C5** · Cs indicate that the size of the alkali metal influences the level of cation-π arene interactions and therefore the conformation of the **Bu^{t}C5** unit; for example, **Bu^{t}C5** · Na has a cone conformation while **Bu^{t}C5** · Cs shows a flattened cone conformation. Cation-π arene interactions are observed in most of the calixarene salts.

1. Introduction

The base-induced condensation of *para*-substituted phenols and formaldehyde produces the calixarene series (Fig. 1), macrocyclic phenol oligomers available in a variety of ring sizes [1].

Calixarenes have myriad applications throughout the field of chemistry. Their cyclic framework, together with the presence of phenol oxygen donor atoms, affords a platform for the complexation of metal atoms [2–6], while the hydrophobic cavity allows the inclusion of charged and neutral organic guests [7–10]. Their chemistry has been applied and explored in catalysis, enzyme mimics, host-guest chemistry, selective ion transport, and sensors [1,2,11]. Calixarenes have been shown to act as versatile building blocks in supramolecular and coordination chemistry, because both their wider (upper) and narrower (lower) rims can be easily modified, at least for the even members of the series (n = 4, 6 or 8) [12]. These modifications (e.g. addition of ester, amide, carboxylic acid, or ketone groups) [7,12–14] have been of great interest in organic and organometallic [5] chemistry of calixarene derivatives.

Deprotonated calixarene derivatives, "calixanions", have also attracted interest in a number of fields. Calixanions can be precursors to functionalized complexes. Certain isolated calixanions have been shown to have interesting layered solid state structures, similar to clays [1,5,11,15,16]. The discovery that the parent calixarenes effect the transport of alkali metal ions in water/organic solvent/water membrane systems has led to particular interest in mono-deprotonated calixanions [17].

In the last two decades, considerable attention has been devoted to the chemical modification of the "major" even membered calix[n]arenes (n = 4, 6, 8), due to their ease of synthesis [2,5,6,11,12]. More recently, progress has also been made in the odd membered calix[n]arenes (n = 5, 7, 9) [4,5,12].

p-tert-Butylcalix[5]arene (**Bu^{t}C5**) is particularly attractive. **Bu^{t}C5** has a cavity size with an ideal balance between constraint and flexibility [18,19], compared to its calix[4,6,8]arene analogues. It is larger and more flexible than calix[4]arene, but it still favors the cone conformation of C_{5v} symmetry [14].

Our interest in calix[5]arene is related to our longer-term research objectives. We are interested in modeling a bifunctional oxo surface, in which two groups can react in a cooperative manner. This requires a conformation that will allow two metals, or a metal and non-metal, to interact on the calixarene "surface". The

* Corresponding author. Fax: +1 817 257 7330.
E-mail address: t.hanna@tcu.edu (T.A. Hanna).

0022-328X/$ - see front matter © 2009 Elsevier B.V. All rights reserved.
doi:10.1016/j.jorganchem.2008.12.065

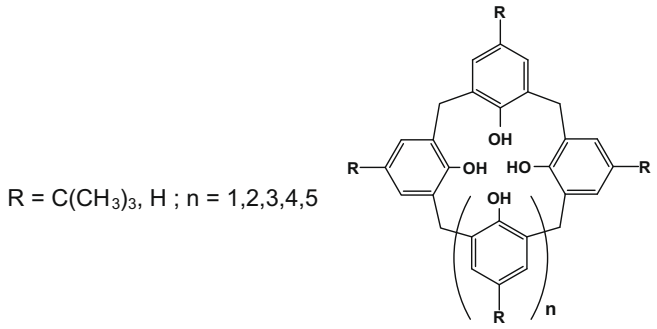

Fig. 1. Calix[4,5,6,7,8]arenes.

calixarene must accommodate both heteroatoms and allow them to interact.

Calix[$n \geq 4$]arenes have the ability to form complexes with alkali metal cations with stoichiometries higher than 1:1 [20–22]. The relatively small cavity of calix[4]arene can disfavor metal–metal interactions due to steric crowding in dimetallocalixarenes, for example by producing a 1,2-alternate conformation [7,23]. If the ring is too large, such as in calix [6,8] arenes, then it is also not possible to observe intramolecular interactions between "guest" heteroatoms [24]. For the intermediate size of calix[5]arene, though, Lattman et al. reported that the oxygen-rich lower rim of **Bu^{t}C5** can accommodate both a ligand [25] (soft donor, phosphorus) and a metal in close proximity, allowing the study of the ligand–metal interaction [26,27]. **Bu^{t}C5** anions could therefore provide precursors for multi-metallic calixarenes [24,28].

In this paper we describe the syntheses and characterization of the alkali metal salts of **Bu^{t}C5** mono-, di-, tri-, and pentaanions, as well as the effects of base strength, alkali metal, and stoichiometry on the structure and deprotonation level of the calixarene ring.

2. Background

Among the calix[n]arene anions reported in literature those for $n = 4$ are the most well represented [20,21,29–32]. In 2003 our group described the synthesis of a large series of mono- and dianionic calixarene alkali metal salts [20,21], observing that the size and nature of the alkali metal has a very important role in the conformation and the characteristics of the calixanions obtained. Solid state structures for monoanionic species (**HC4** · Li, **HC4** · Na, **HC4** · Rb, **HC4** · Cs) exhibit the cone conformation while the dianionic species [e.g. **HC6** · M_2 (M = K, Rb, Cs)] contain calixarenes in a flattened 1,2,3-alternate conformation. We also demonstrated the utility of calix[4]anions as an entry into both main-group (the first antimony calixarene [33]) and transition metal calixarene complexes [34] that were inaccessible using the traditional parent calixarene as precursor.

Information about **Bu^{t}C5** anions, in contrast, is very limited. Titration of **Bu^{t}C5** with Et_3N in acetonitrile provided the spectrophotometric determination of the first two pK_a values of the calixarene ammonium salt (pK_{a1} = 11.5 ± 0.7; pK_{a2} = 15.4 ± 1.0) [35]. This data led to the preparation of trianionic **Bu^{t}C5** and the further isolation of **Bu^{t}C5** lanthanide(III) complexes [35].

Gutsche and coworkers reacted **Bu^{t}C5** and $KHCO_3$ in a 1:1 ratio to generate the potassium monoanionic salt of **Bu^{t}C5** *in situ*. This **Bu^{t}C5** · K salt was used as precursor for the preparation of lower rim monosubstituted derivatives of **Bu^{t}C5**. No isolation or characterization of the monoanion salt was performed [36]. Pentaalkyl ester derivatives of *p*-benzylcalix[5]arene (**BnC5**) were synthesized by Asfari and coworkers from the reaction of **BnC5** with an excess of K_2CO_3 (to produce the anion precursor), followed by addition of the alkylating agent to yield the desired substituted calixarene [37].

Some metallocalixarenes have been also obtained by the use of **Bu^{t}C5** anionic salt precursors in one-pot reactions. An unsymmetrical dimeric 1:1 K/Ti complex was achieved by the reaction of **Bu^{t}C5** with potassium followed by [Ti(acac)(OPr^i)$_2$] [38]. The solid state structure showed a central Ti–O–Ti core with an encapsulated K^+ ion on each **Bu^{t}C5** unit.

The crystal structures of the Na^+ and Rb^+ salts of a functionalized calix[5]arene were obtained by McKervey and coworkers during extraction studies of chemically modified calix[5]arenes [14]. No crystal structures of lithium or cesium salts of **Bu^{t}C5** have been reported.

Clearly the systematic isolation, study, and full characterization of the anionic salts of **Bu^{t}C5** is lacking. In most cases where **Bu^{t}C5** anions are prepared the level of deprotonation and conformation of the parent calixarene remains ambiguous. The objective of this work is to study the interaction and conformational behavior of **Bu^{t}C5** anions with one or more alkali atoms within the framework.

3. Results and discussion

3.1. Synthesis of monoanions

Alkali metal salts of monoanionic **Bu^{t}C5** were obtained with several bases in 72–86% yields (Scheme 1). It is important to control the base stoichiometry and strength. Alkali salt monoanions are easily obtained from the reactions of **Bu^{t}C5** with 1 equivalent of MOC(CH$_3$)$_3$ (M = Na, K), NaH, or with M_2CO_3 (M = Na, K, 1 equivalent; Rb, Cs 0.5 equivalents). Reactions with MOC(CH$_3$)$_3$ and NaH are faster than the ones with M_2CO_3. The crude material is washed in pentane (or hexane) and suitable X-ray quality crystals are obtained by the slow evaporation of the concentrated THF or MeCN solution.

As we previously reported, the reaction of calix[6]arene (**Bu^{t}C6**) with 1 equivalent of M_2CO_3 leads to the preparation of calix[6]arene dianions [20]. For **Bu^{t}C5**, when the reaction ratio of the M_2CO_3 (M = Na, K) salt was increased from 0.5 to 1–3 equivalents, the product obtained was surprisingly the monoanionic salt but in better yields. The best yield was obtained when using 1 equivalent of the carbonate salt (72–82% yield). These results could be due to the low solubility of the metal carbonates in THF or MeCN. In an attempt to produce the dianionic salts, we increased the solubility of the carbonates by using a mixture of C_6H_6/MeOH, however the reaction still yields the monoanionic salts of **Bu^{t}C5**.

The synthesis of the lithium monoanion using Li_2CO_3 was unsuccessful due to its poor solubility. The use of LiH provides the monoanionic salt but in mixture with the trianionic complex. Isolation of the monoanionic salt **Bu^{t}C5** · Li from the mixture is difficult because it decomposes easily in solution to the parent calixarene.

Rubidium and cesium salts **Bu^{t}C5** · M were obtained from the reaction of **Bu^{t}C5** and 1 equivalent of MOH or 0.5 equivalent of M_2CO_3 (M = Rb, Cs) under reflux. Pure monoanionic salts were obtained as colorless block crystals when the crude material was recrystallized by diffusion of pentane into its concentrated THF solution.

Most of the alkali metal salts of the **Bu^{t}C5** monoanions are quite air and moderately moisture stable. In all cases the preparation of the single crystals was performed under air.

3.2. Synthesis of dianions

Although treatment of **Bu^{t}C5** with M_2CO_3 led to monoanions **Bu^{t}C5** · M (M = Na, K), the same strategy led to the formation of dianions when M = Rb, Cs were used. When **Bu^{t}C5** was treated with Rb_2CO_3 or Cs_2CO_3 in a 1:1 molar ratio the resulting salts were

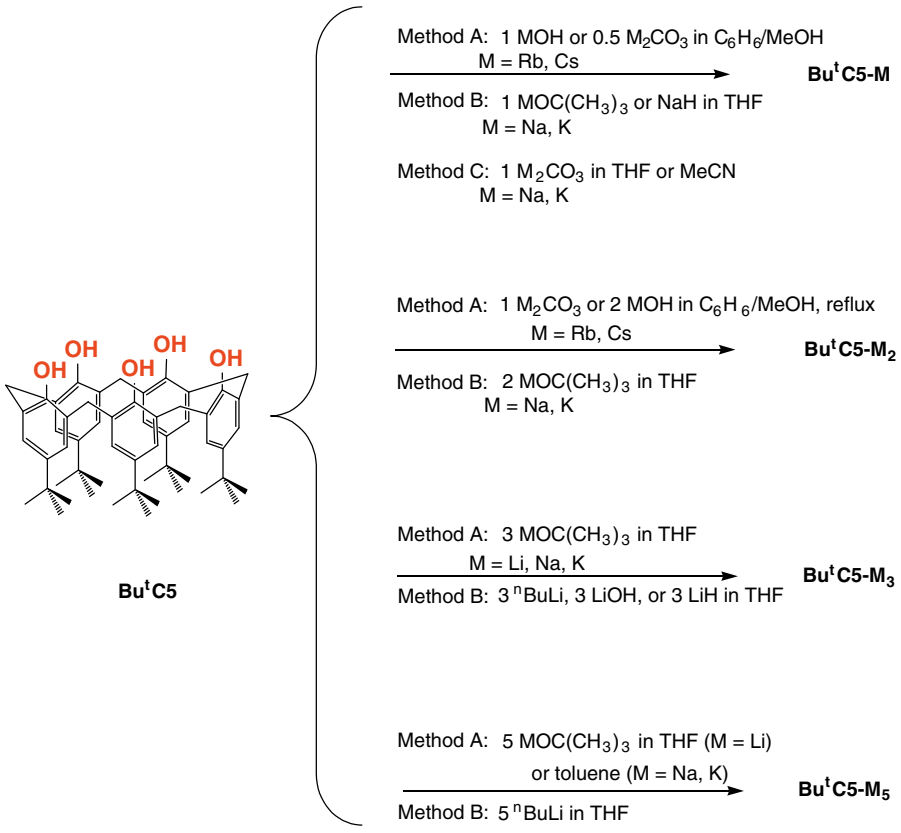

Scheme 1. Synthesis of **Bu^{t}C5** anions.

the dianionic species **Bu^{t}C5** · M_2 (M = Rb, Cs), obtained in good yield (81–83%) (Scheme 1). These results can be explained by the better solubility of the Rb and Cs carbonates in the C_6H_6/MeOH mixture. **Bu^{t}C5** · M_2 salts could also be obtained from the reaction of **Bu^{t}C5** and MOH (M = Rb, Cs) in a 1:2 ratio. The pure products can be isolated as colorless crystals by diffusion of pentane into the concentrated THF solutions.

When **Bu^{t}C5** was treated with $MOC(CH_3)_3$ (M = Na, K) in a 1:2 ratio, the resulting salts were the dianionic species **Bu^{t}C5** · M_2 obtained in good yields (92–96%). The products were purified by washing the crude product with pentane. X-ray quality crystals of the **Bu^{t}C5** · K_2 salt could be obtained by slow evaporation of a THF and DMSO mixture (10:1 ratio). Stoichiometry in this reaction plays an important role since a small excess of the alkali *tert*-butoxide could afford a mixture of di- and trianionic salts.

We attempted to synthesize the lithium dianion following the same strategy as for the Na and K dianionic salts using lithium *tert*-butoxide, however, in all cases we observed the formation of the trianionic species **Bu^{t}C5** · Li_3 in mixture with parent calixarene.

Bu^{t}C5 · K_2 and **Bu^{t}C5** · Na_2 are white powders, which after 4 days in air start to decompose to green powders. **Bu^{t}C5** · Rb_2 and **Bu^{t}C5** · Cs_2 are quite air stable, but they start to release the parent calixarene after 2 months in air.

3.3. Synthesis of trianions

The reported pK_a values of **Bu^{t}C5** (pK_{a1} = 11.5, pK_{a2} = 15.4) [35], suggested that the most suitable way to obtain the trianionic species would be the use of strong alkali metal bases. Indeed, we found that the use of alkali metal *tert*-butoxides easily yields the trianionic salts of **Bu^{t}C5** (Scheme 1).

Reaction of **Bu^{t}C5** with $MOC(CH_3)_3$ or MOH (M = Li, Na, K) in a 1:3 ratio in THF at room temperature produces the respective trianionic salts. When $MOC(CH_3)_3$ was used, the products were easily isolated by crystallization of the crude material (71–97% yields); however, isolation of the product was more difficult when MOH was used. LiH and Bu^{n}Li also produced the calixarene trianion even working with just 1 equivalent of base (the remaining product is unreacted **Bu^{t}C5**). The use of 5 equivalents of LiH gave the best yield of **Bu^{t}C5** · Li_3 (97%) while 3 equivalent of Bu^{n}Li produced **Bu^{t}C5** · Li_3 in 86% yield. The pure products are air stable white powders, but they start to decompose to parent **Bu^{t}C5** after 5 weeks in air.

3.4. Synthesis of pentaanions

When **Bu^{t}C5** was treated in a 1:5 molar ratio with $MOC(CH_3)_3$ (M = Li, Na, K) or ^{n}BuLi the penta-deprotonated **Bu^{t}C5** · M_5 salts were obtained in 77–91% yields (Scheme 1). The selection of the right solvent is very important in these reactions. When **Bu^{t}C5** was treated with $MOC(CH_3)_3$ in THF, a mixture of **Bu^{t}C5** · M_3 and **Bu^{t}C5** · M_5 (M = Na, K) was obtained, but when the solvent was switched to toluene, pure **Bu^{t}C5** · M_5 was obtained. In a similar way when $LiOC(CH_3)_3$ was reacted with **Bu^{t}C5** in toluene a mixture of tri- and pentaanion was obtained. In this case THF was necessary for the preparation of pure product.

Attempts to synthesize tetranionic salts **Bu^{t}C5** · M_4 by the reaction of **Bu^{t}C5** and $MOC(CH_3)_3$ (M = Li, Na, K) in a 1:4 ratio were unsuccessful, yielding a mixture of the tri- and pentaanionic salts of **Bu^{t}C5**.

3.5. NMR spectroscopy

^{1}H NMR spectral patterns reveal calixarene conformations and VT-NMR is used to determine inversion rates. The room temperature ^{1}H NMR spectra for the mono- (Fig. 2) and dianionic salts

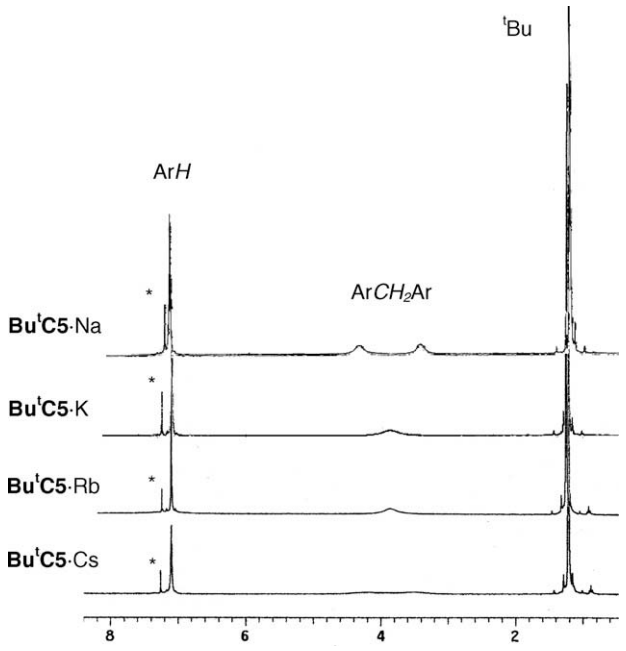

Fig. 2. ^{1}H NMR spectra of alkali metal salts of the monoanionic **Bu^{t}C5** in $^*CDCl_3$.

(Fig. 3) show similar patterns. The chemical shifts for aromatic protons in **Bu^{t}C5** · M and **Bu^{t}C5** · M_2 (M = Na, K, Rb, Cs) shift upfield to 6.97–7.18 ppm in $CDCl_3$ as sharp singlets integrating to 10 H atoms (the chemical shift for aromatic protons in **Bu^{t}C5** is at 7.21 ppm). The methylene region shows two broad signals between 4.37 and 2.85 ppm in the case of **Bu^{t}C5** · M and **Bu^{t}C5** · M_2 (M = Na, Cs) and one broad signal between 3.86 and 3.77 ppm for **Bu^{t}C5** · M and **Bu^{t}C5** · M_2 when M = K, Rb. The broadness of the methylene signals indicates fluxionality of the complexes in solution [39]. The *tert*-butyl resonances in all mono- and dianionic salts appear as sharp singlets between 1.18 and 1.23 ppm.

The behavior of the OH groups for the mono- and dianionic salts has strong dependence on the solvent and alkali metal. Signals for OH groups in the monoanions, for example, were only observed for the **Bu^{t}C5** · K and **Bu^{t}C5** · Cs salts (at 8.66 and 8.75 ppm, respectively) when the NMR spectra were taken in $CDCl_3$ at room temperature. The OH groups for the **Bu^{t}C5** · Na and **Bu^{t}C5** · Rb salts in this solvent are too broad to be observed at rt. In the case of the dianions, OH signals are only found for the **Bu^{t}C5** · Rb_2 and **Bu^{t}C5** · Cs_2 salts (8.03 and 13.49 ppm, respectively) when the solvent used is $CDCl_3$, but if we change the NMR solvent from $CDCl_3$ to DMSO-d_6, the OH signals for **Bu^{t}C5** · Na_2 and **Bu^{t}C5** · K_2 can be located at 15.38 and 15.15 ppm, respectively. This NMR behavior highlights the previously observed [in even numbered calix[*n*]arene salts (*n* = 4, 6, 8)] influence of the solvent polarity in the rate of conformational inversion of calixanions [20].

^{13}C NMR spectra of all the mono and dianionic salts show four peaks for the aromatic carbons, one peak for the methylene groups and two peaks for *tert*-butyl groups. In the ^{13}C spectra the signals at about 34 ppm are assigned to the ArCH_2Ar groups. The simplicity of the ^{1}H NMR, and the single methylene peak in the ^{13}C spectra for the mono and dianionic salts, are typical of cone structures in the solution state, consistent with the solid state structures (vide infra) [36].

The ^{1}H NMR spectra of trianionic salts of **Bu^{t}C5** (Fig. 4) show patterns that are very different from those of the mono- and dianionic salts. In the case of the potassium trianion **Bu^{t}C5** · K_3 the aromatic protons are present as a single peak at 7.69 ppm, while the ArCH_2Ar protons show two doublet signals at 3.45 and 4.29 ppm. The presence of this pair of doublets indicates a loss in fluxionality of **Bu^{t}C5** · K_3 in comparison with mono and dianionic salts. The *tert*-butyl group appears as a singlet at 1.51 ppm. The ^{13}C NMR spectrum shows four signals for aromatic carbons, one for methylene and two for *tert*-butyl groups. This NMR pattern is consistent with a cone conformation of **Bu^{t}C5** · K_3 in solution.

The spectra of the lithium and sodium trianionic salts are more complex. The **Bu^{t}C5** · Li_3 salt shows three sharp singlets from 7.22

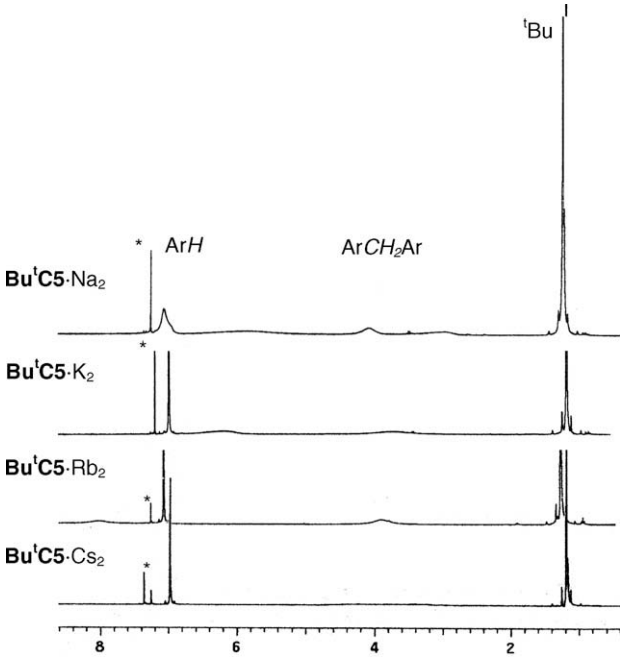

Fig. 3. ^{1}H NMR spectra of alkali metal salts of the dianionic **Bu^{t}C5** complexes in $^*CDCl_3$.

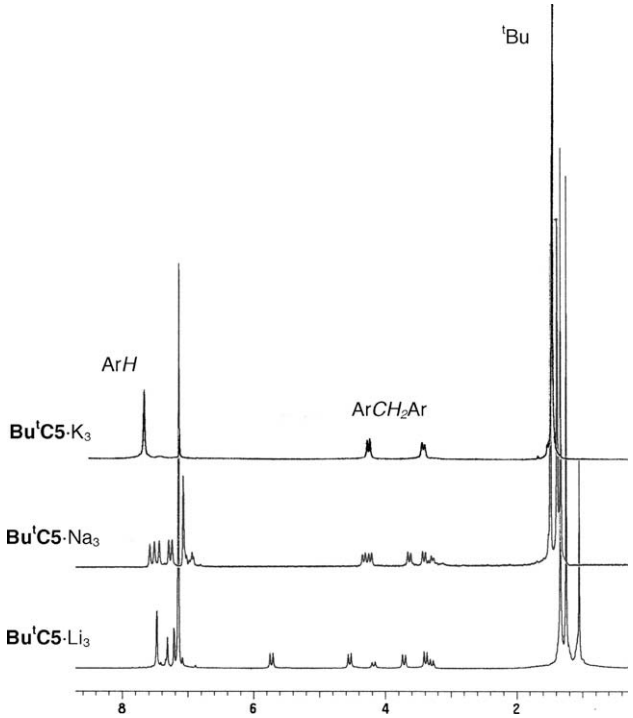

Fig. 4. ^{1}H NMR spectra of alkali metal salts of the trianionic **Bu^{t}C5** complexes in C_6D_6.

Table 1
Coalescence temperatures at 300 MHz and free energies of activation for the conformational inversion of **Bu^{t}C5** and **Bu^{t}C5** anions.

Compound	T_c (°C)	$\Delta\nu$/(±15) (Hz)	$\Delta G^{\mp}$/(±0.4) (kcal mol^{-1})
Bu^{t}C5 [36]	271		13.2
Bu^{t}C5 · Na	276	280	12.6
Bu^{t}C5 · K	278	184	12.9
Bu^{t}C5 · Rb	280	255	12.8
Bu^{t}C5 · Cs	301	182	14.1
Bu^{t}C5 · Na_2	323	182	15.1
Bu^{t}C5 · K_2	291	224	13.4
Bu^{t}C5 · Rb_2	278	297	12.7
Bu^{t}C5 · Cs_2	300	339	13.6

to 7.48 ppm in the aromatic area, while **Bu^{t}C5** · Na_3 exhibits five singlets from 7.33 to 7.67 ppm. Both the lithium and sodium salts produce six doublets (geminal coupling due to nonequivalent methylene hydrogens) for the methylene protons with two doublets being half the intensity of the others. This spectrum is a good indication of an overall C_s symmetry for the molecule and a probable 1,2 or 1,3-alternate, or partial cone conformation [36]. The *tert*-butyl area shows three singlet peaks in a 2:2:1 ratio probably due to the fact that the three alkali metals in the ring restrict the free rotation of phenolic groups in the annulus. The ^{13}C spectrum for **Bu^{t}C5** · Na_3 was not possible due to insufficient solubility.

The solution ^{1}H NMR spectra of pentaanionic **Bu^{t}C5** salts are very similar. All of them show a single peak for aromatic protons, one *tert*-butyl peak and a pair of sharp doublets in the methylene area. The simplicity and sharp peaks in NMR permit the average solution structures to be assigned as cone conformation.

3.5.1. Conformational studies

Bu^{t}C5 resembles calix[4]arene with four basic conformations (cone, partial cone, 1,2-alternate, 1,3-alternate), but generally inverts more easily due to its wider annulus [36]. Variable temperature ^{1}H NMR spectra for the salts **Bu^{t}C5** · M (M = Na, K, Rb, Cs) and **Bu^{t}C5** · M_2 (M = Na, K, Rb, Cs) led to their coalescence temperatures, and the energies ($\Delta G^{\mp}$) for the conformational interconversion were calculated (Table 1).

3.5.2. Inversion energies

The room temperature ^{1}H NMR spectrum of **Bu^{t}C5** exhibits a broad peak close to coalescence for the methylene groups that bridge the arene units (ArCH_2Ar), indicating that the two types of protons of the cone conformer are exchanging environments on the NMR time scale. We also observe a single broad signal in the room temperature NMR spectra of the salts **Bu^{t}C5** · M and **Bu^{t}C5** · M_2 (M = K, Rb), but the spectra of **Bu^{t}C5** · M and **Bu^{t}C5** · M_2 (Na, Cs) show a pair of broad signals. The calixanions are likewise in cone conformation, but the inversion is slightly less rapid in **Bu^{t}C5** · M and **Bu^{t}C5** · M_2 (Na, Cs) than in the parent molecule.

The **Bu^{t}C5** · M salts for M = Na, K, Rb have similar $\Delta G^{\mp}_{inv}$ values to that of the parent calixarene. This result is surprising since it was

Table 2
Selected M–O and M–C distances of alkali metal salts of calixanions.

Compound	M–O (OAr) (Å)	M–O (solvate) (Å)	M–C (Å)[a]	Ref.
Monoanions				
Na salts				
[**Bu^{t}C5** · Na · THF]$_2$	2.336(2)–2.973(2)	2.332(3)		[b]
(**HC4** · Na)$_2$ · 3Me_2CO	2.305(6)–2.359(6)	2.217(6)–2.441(7)		[20]
(**HC4** · Na)$_2$ · 3Me_2CO	2.284(5)–2.337(5)	2.206(6)–2.394(5)		[31]
[Bu^{t}C5 · Na · MeCN]$_2$	2.325(3)–2.696(3)			[b]
K salts				
Bu^{t}C5 · K · MeCN	2.670(2)–2.974(2)		3.355(3)–3.390(3)	[b]
HC4 · K · 1.5H_2O · THF	2.743(3)–2.893(2)	2.656(4)–2.845(3)	3.286(3)–3.515(3)	[21]
Bu^{t}C4 · K · 4THF	3.042(13)–3.160(12)	2.648(13)–2.728(11)		[21]
[**Bu^{t}C4** · K · 2THF · H_2O]$_2$	2.737(2)–2.935(2)	2.694(2)–2.733(2)		[21]
Rb salts				
Bu^{t}C5 · Rb · THF	2.870(6)–3.241(7)	2.919(8)	3.263(9)–3.494(9)	[b]
Bu^{t}C4 · Rb · 4THF	3.124(2)	2.796(2)		[20]
HC4 · Rb · THF	2.943(3)	2.7770(17)	3.349(3)–3.579(3)	[20]
Cs salts				
Bu^{t}C5 · Cs · THF	3.015(4)– 3.352(4)	3.063(5)	3.368(5)– 3.715(6)	[b]
HC4 · Cs · Me_2CO	3.100(3)	2.959(3)	3.599(3)–3.840(3)	[20]
HC4 · Cs · pyridine	3.169(12)–3.704(16)		3.53(1)–4.17(1)	[31]
HC4 · Cs · H_2O	3.065(5)–3.673(5)	2.97(3)	3.530(7)	[31]
Bu^{t}C4 · Cs · MeCN	~4.0		3.545(3)–3.961(3)	[30]
HC6 · Cs · Me_2CO	3.073(12)–3.535(15)	2.99(2)	3.416(15)–3.886(16)	[20]
Dianions				
[**Bu^{t}C5** · K_2 · 4DMSO]$_2$	2.655(8)– 2.838(8)	2.587(9)– 2.776(9)		[b]
HC6 · K_2 · 2Me_2CO	2.805(2)–3.056(3)	2.699(3)–2.981(3)	3.214(3)–3.713(3)	[20]
HC6 · K_2 · 5MeOH	2.64(1)–2.94(1)	2.74(1)–2.91(1)	3.28(2)–3.96(2)	[40]
[**Bu^{t}C5** · Rb_2 · 2THF · H_2O]$_2$	2.820(3)– 3.294(3)	2.615(14)–2.975(5)	3.329(4)–3.478(5)	[b]
HC6 · Rb_2 · 2Me_2CO	2.986(2)–2.999(3)	2.835(4)–3.095(4)	3.304(4)–3.731(4)	[20]
[**Bu^{t}C5** · Cs_2 · 2THF · 2H_2O]$_2$	2.959(3)– 3.457(3)	2.869(11)– 3.191(9)	3.454(4)– 3.642(4)	[b]
HC6 · Cs_2 · 2Me_2CO	2.975(12)–3.000(8)	2.853(10)–3.093(9)	3.301(13)–3.728(13)	[20]
Trianions				
[**Bu^{t}C5** · Li_3 · 3THF · H_2O]$_2$	1.887(10)–2.000(11)	1.836(16)–2.001(11)	2.700(17)	[b]
[**Bu^{t}C5** · Li_3 · 2THF · 2H_2O]$_2$	1.905(7)– 2.064(8)	1.872(8)–1.995(10)	2.677(10)– 2.686(11)	[b]
[**Bu^{t}C5** · Na_3 · 2THF]$_2$	2.211(3)–2.995(4)	2.245(4)–2.262(6)	2.739(4)– 3.031(4)	[b]
Bu^{t}C5 · Na_3 · THF · 4DMSO	2.290(4)–2.737(3)	2.251(3)– 2.409(3)	2.979(6)	[b]

[a] Distances for cation-π arene interactions.
[b] This work.

expected that the presence of an alkali metal in the calixarene would increase the rigidity of the ring, as was previously observed for **HC4**, **HC6** and **Bu^{t}C6** [20]. The **Bu^{t}C5** · Cs salt is the only monoanion to show increased rigidity, with a $\Delta G^{\mp}_{inv}$ value of 14.1 ± 0.4 kcal mol^{-1}, and a pair of broad signals for the $ArCH_2Ar$ groups.

Likewise, we expected that two metals in the cavity would lead to much higher $\Delta G^{\mp}_{inv}$ values for the dianionic salts compared to that of the parent calixarene. The data, however, showed that **Bu^{t}C5** · M_2 (M = K, Cs) salts have $\Delta G^{\mp}$ values similar to those of parent calix[5]arene and the monoanionic salts. The **Bu^{t}C5** · Na_2 salt is the only dianion showing a higher $\Delta G^{\mp}$ value (15.1 ± 0.4 kcal mol^{-1}), indicating less conformational mobility and a probable dimeric structure (as observed in the solid state).

All of the energy differences are rather small, though, and we have noted other factors that influence the ^{1}H NMR patterns of the salts. Water or residual solvent leads to changes in the methylene area, probably due to interactions with either the cation or phenol groups of the calixarene. The high solvent sensitivity could be a reason for the unexpected values observed in our VT-NMR studies.

3.5.3. Crystal structures of the calixanions

The crystal structures of **Bu^{t}C5** · M (M = Na, K, Rb, Cs), **Bu^{t}C5** · M_2 (M = K, Rb, Cs) and **Bu^{t}C5** · M_3 (M = Li, Na) were obtained. To our knowledge these are the first reported examples of solid state structural characterization for **Bu^{t}C5** anions. Bond distances and angles fall within normal parameters, as can be seen from Table 2.

3.5.4. Metal–oxygen versus metal–carbon (π-cation) interactions

The **Bu^{t}C5** series allows us to examine the relative affinities of each metal for interaction with the phenolic oxygens on the calixarene lower rim versus π-cation interactions with the arene rings within the cavity. A combination of these effects determines the following structure types:

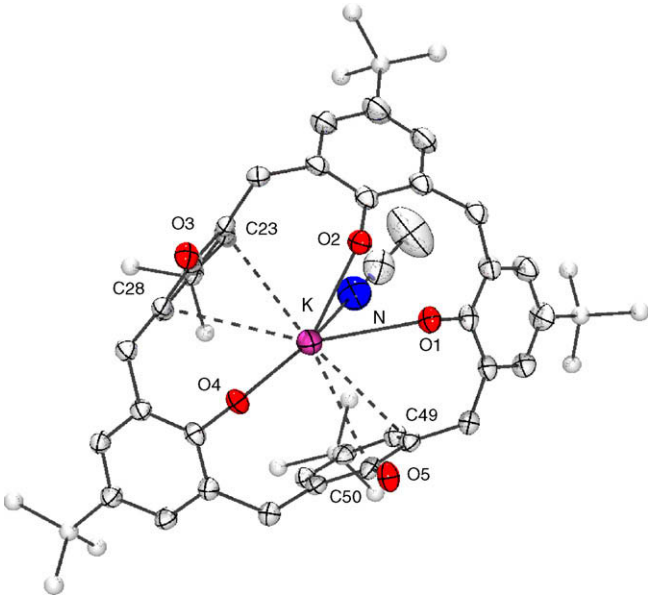

Fig. 5. Crystal structure of monomeric **Bu^{t}C5** · K · MeCN. Thermal ellipsoids are shown at 50% probability; hydrogen atoms and noncoordinated solvent molecules are omitted for clarity.

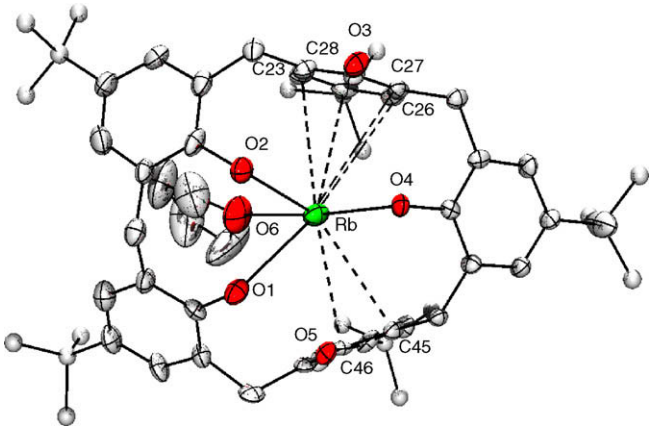

Fig. 6. Crystal structure of monomeric **Bu^{t}C5** · Rb · THF. Thermal ellipsoids are shown at 50% probability; hydrogen atoms are omitted for clarity.

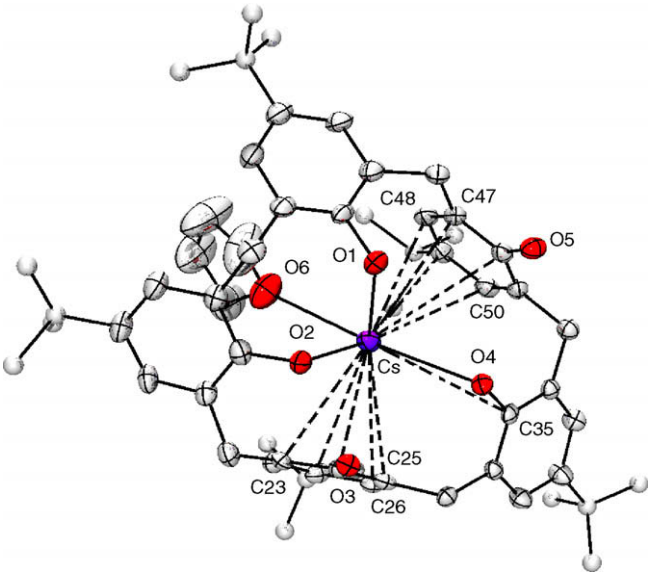

Fig. 7. Crystal structure of monomeric **Bu^{t}C5** · Cs · THF. Thermal ellipsoids are shown at 50% probability; hydrogen atoms are omitted for clarity.

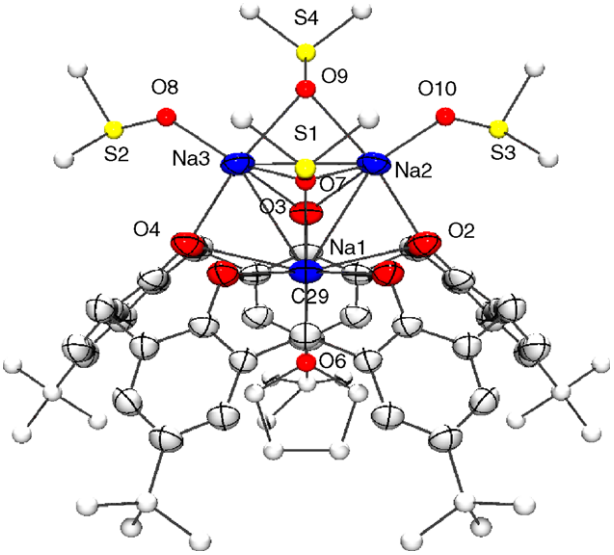

Fig. 8. Crystal structure of monomeric **Bu^{t}C5** · Na_3 · THF · 4DMSO. Thermal ellipsoids are shown at 50% probability; hydrogen atoms are omitted for clarity.

3.5.4.1. Discrete monomeric units. **Bu^{t}C5** · K · MeCN (Fig. 5) exhibits a monomeric structure with coordination of the potassium atom to three phenolic oxygens in the calixarene ring and one acetonitrile molecule. The conformation of the calixarene unit is flattened cone due to M–C π interactions. **Bu^{t}C5** · M · THF (M = Rb, Cs) also exhibit monomeric structures (Figs. 6 and 7) with the calixarene in flattened cone conformation consistent with the ^{1}H NMR patterns observed in solution. Rubidium and cesium show a greater number of M–C calixarene interactions compared to potassium. In all these complexes the bulky *tert*-butyl groups block the formation of polymeric structures [31].

The X-ray structure of **Bu^{t}C5** · Na_3 · THF · 4DMSO (Fig. 8) shows a monomeric unit containing three sodium atoms located in the lower rim of the calixarene ring. A THF molecule was located inside the cavity, blocking the possible Na1-π arene interactions, while four DMSO solvate molecules are coordinated to the two exo sodium atoms (Na2 and Na3).

3.5.4.2. Discrete dimeric units. The **Bu^{t}C5** · Na · S (S = THF, MeCN) dimers (Fig. 9) contain an inversion center located halfway between the two sodium atoms. The structure does not show any π-cation interaction probably because of the small cation and its location on the lower rim, and the calixarene is in the cone conformation. Dimeric structures are also observed for **Bu^{t}C5** · M_2 (M = K, Rb, Cs) and **Bu^{t}C5** · M_3 (M = Li, Na).

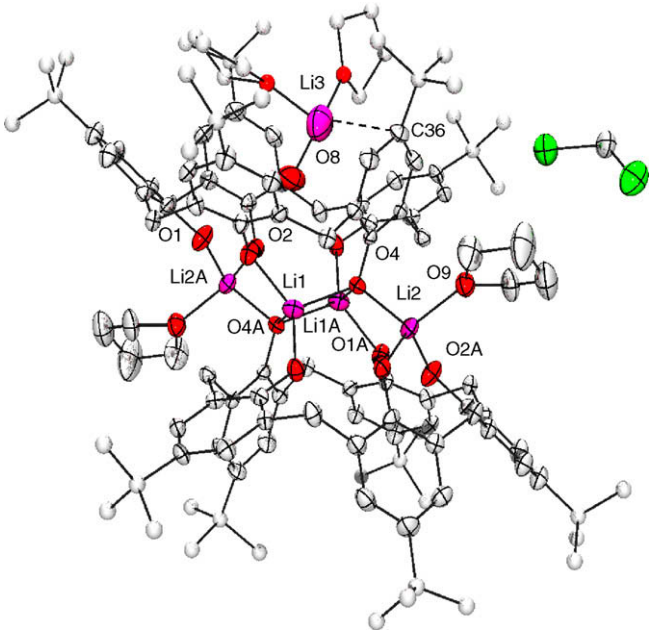

Fig. 10. Crystal structure of dimeric **Bu^{t}C5** · Li_3 · 3THF · H_2O. Thermal ellipsoids are shown at 50% probability; hydrogen atoms and third lithium of second ring are omitted for clarity.

3.5.5. Core structures

3.5.5.1. Lithium. Li aryloxides have a rich coordination chemistry with a predilection toward multinuclear clusters and Li–O–Li bridges [41–43]. The two **Bu^{t}C5** · Li_3 complexes are quite similar; we will discuss only [**Bu^{t}C5** · Li_3 · 3THF · H_2O]$_2$ (Fig. 10). The dimeric crystal structure of complex [**Bu^{t}C5** · Li_3 · 3THF · H_2O]$_2$ includes two different lithium atoms located in the lower rim of the calixarene unit (Li1 and Li2). The first lithium atom (Li1) is oxo-bridged to a second one (Li1A) by one phenolic oxygen (O4A) from each calixarene unit, forming a four membered $Li_2(\mu\text{-}O)_2$ core structure with Li–O distances of 1.973(11) Å and 1.993(11) Å. The Li–O–Li and O–Li–O angles are 80.7(5)° and 99.3(5)°, respectively. The second lower rim lithium atom (Li2) has a pseudo tetrahedral geometry with coordination to two phenolic oxygen atoms (O1 and O2) from the first ligand, one THF molecule and a phenolic oxygen (O4A) from the second calixarene. It can be observed that O4 triply bridges Li1, Li1A, and Li2, while O4A bridges Li1, Li1A, and Li2A. The overall Li/O core structure in complex [**Bu^{t}C5** · Li_3 · 3THF · H_2O]$_2$ is similar to the one observed in the known dianionic **Bu^{t}C4** · Li_2 · $2Me_2CO$ salt [20,44].

An interesting feature of complex [**Bu^{t}C5** · Li_3 · 3THF · H_2O]$_2$ is the fact that the third lithium (Li3) atom is located in the hydrophobic cavity of the **Bu^{t}C5** rings rather than being coordinated to the harder oxygen lower rim. The Li3 atom is coordinated to two THF molecules, one water molecule, and has a long-range interaction with C36 [2.700(17) Å] to give an overall tetrahedral geometry.

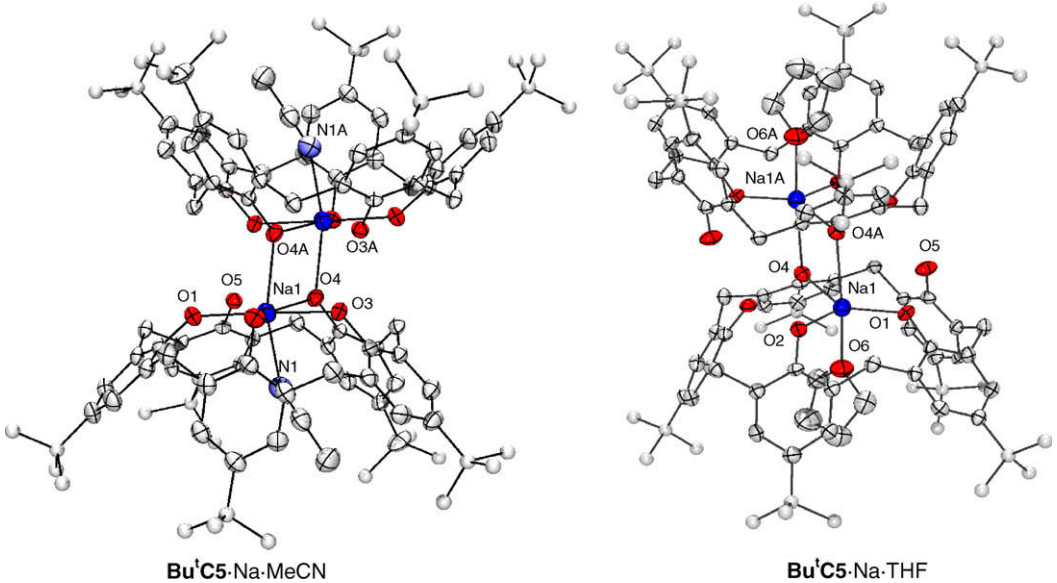

Bu^{t}C5·Na·MeCN **Bu^{t}C5**·Na·THF

Fig. 9. Crystal structures of dimeric **Bu^{t}C5** · Na · S. Thermal ellipsoids are shown at 50% probability; hydrogen atoms and noncoordinated solvent molecules are omitted for clarity.

While the ^{1}H NMR spectrum of **Bu^{t}C5** · Li_3 suggests a 1,2 or 1,3-alternate conformation, the calixarene rings in [**Bu^{t}C5** · Li_3 · 3THF · H_2O]$_2$ are in the flattened cone conformation. This conformation is adopted not because of M–C interactions but due to the steric hindrance of the solvent molecules and the number of alkali metals in the structure.

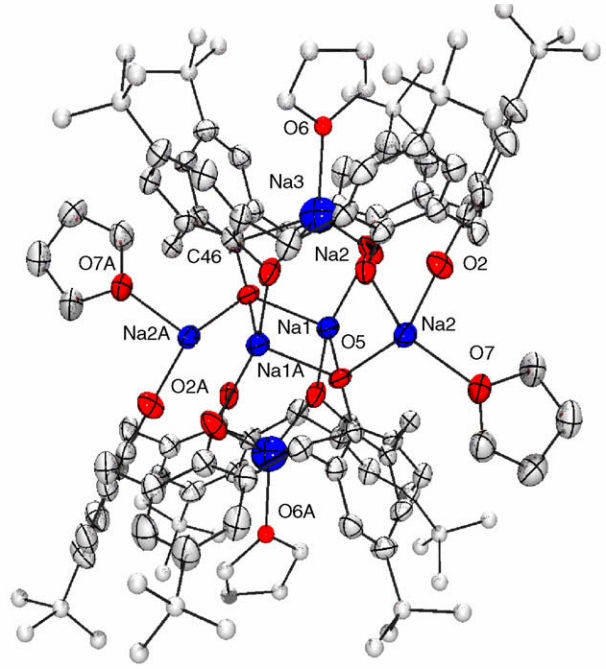

Fig. 11. Crystal structure of dimeric **Bu^{t}C5** · Na_3 · 2THF. Thermal ellipsoids are shown at 50% probability; hydrogen atoms are omitted for clarity.

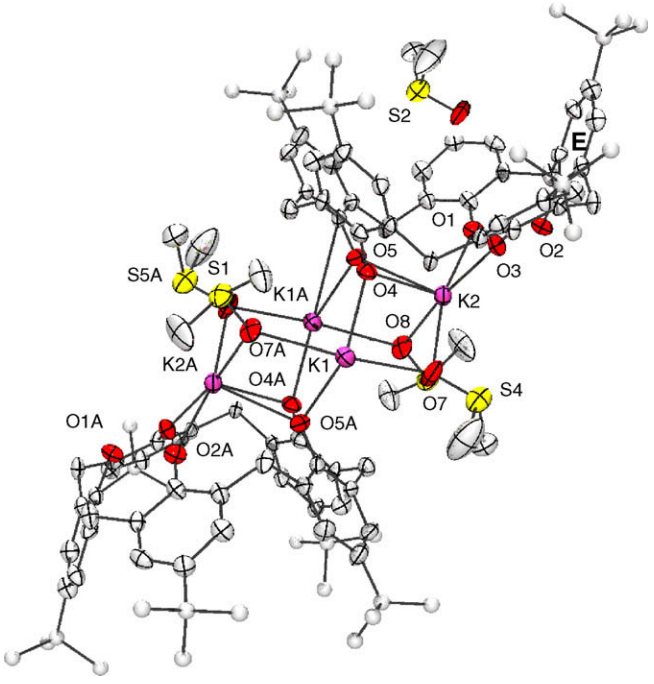

Fig. 12. Crystal structure of dimeric **Bu^{t}C5** · K_2 · 4DMSO. Thermal ellipsoids are shown at 50% probability; hydrogen atoms and noncoordinated DMSO molecules are omitted for clarity.

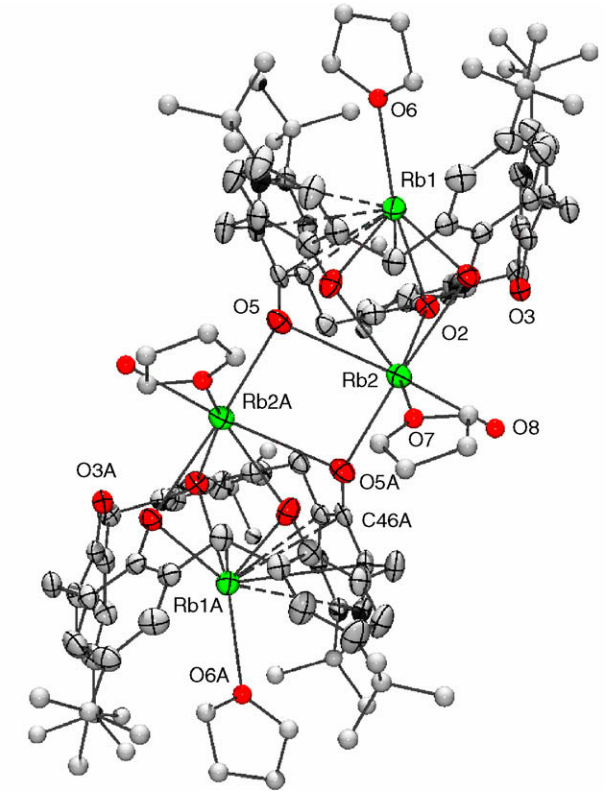

Fig. 13. Crystal structure of dimeric **Bu^{t}C5** · Rb_2 · 2THF · H_2O. Thermal ellipsoids are shown at 50% probability; hydrogen atoms are omitted for clarity.

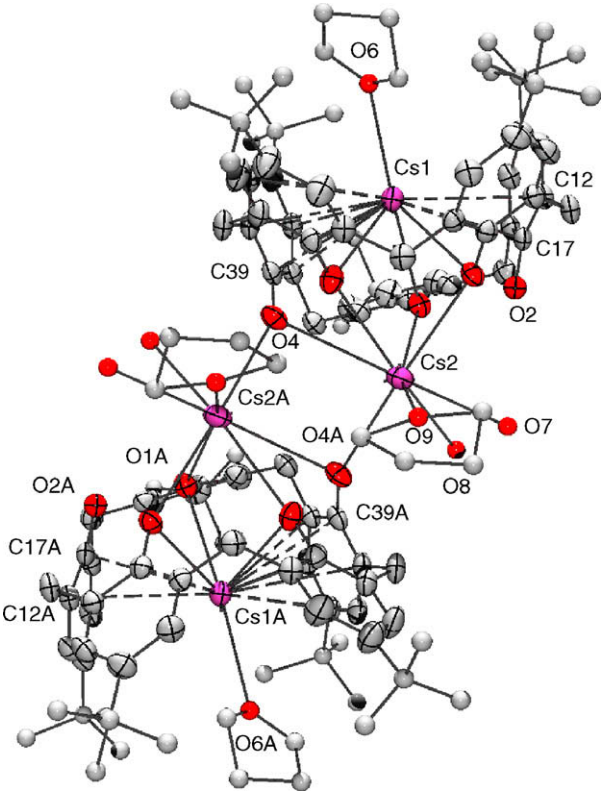

Fig. 14. Crystal structure of dimeric **Bu^{t}C5** · Cs_2 · 2THF · $2H_2O$. Thermal ellipsoids are shown at 50% probability; hydrogen atoms are omitted for clarity.

Table 3
Crystallographic data and summary of data collection and structure refinement.

	[Bu^{t}C5 · Na · THF]$_2$ · C_5H_{12}	**[Bu^{t}C5** · Na · MeCN]$_2$ · 3MeCN	**[Bu^{t}C5** · K · MeCN] · MeCN	**Bu^{t}C5** · Rb · THF	**Bu^{t}C5** · Cs · THF	**[Bu^{t}C5** · K_2 · 4DMSO]$_2$ · 8DMSO
Formula	$C_{123}H_{166}Na_2O_{12}$	$C_{120}H_{153}N_5Na_2O_{10}$	$C_{59}H_{75}KN_2O_5$	$C_{59}H_{77}O_6Rb$	$C_{59}H_{77}O_6Cs$	$C_{142}H_{232}K_4O_{26}S_{16}$
Formula weight	1882.61	1871.51	931.34	967.68	1015.12	3024.81
Crystal system	Triclinic	Triclinic	Triclinic	Monoclinic	Monoclinic	Monoclinic
Space group	$P\bar{1}$	$P\bar{1}$	$P\bar{1}$	$P2_1/c$	$P2_1/c$	$P2_1/n$
T (K)	213(2)	218(2)	218(2)	223(2)	223(2)	213(2)
a (Å)	12.6599(13)	13.5128(10)	12.333(3)	16.657(2)	16.6321(10)	14.440(4)
b (Å)	16.0093(16)	18.0249(13)	13.352(4)	21.062(3)	21.3979(13)	17.897(4)
c (Å)	16.8202(17)	24.6368(18)	17.870(5)	19.198(2)	19.1894(11)	32.661(8)
α (°)	103.727(2)	91.401(2)	81.001(5)	90	90	90
β (°)	103.495(2)	94.0300(10)	76.788(5)	108.944(2)	108.7050(10)	94.166(5)
γ (°)	106.933(2)	110.029(2)	84.162(4)	90	90	90
V (A^3)	2995.6(5)	5616.3(7)	2822.9(13)	6370.8(13)	6468.6(7)	8418(4)
Z	1	2	2	4	4	2
$d_{calcd.}$ (g cm^{-3})	1.004	1.099	1.092	1.009	1.042	1.193
μ (mm^{-1})	0.069	0.0760	0.140	0.818	0.612	0.364
Reflections collected	12957	15760	16891	43091	74471	53275
T_{min}/T_{max}	0.986	0.985	0.973	0.858	0.890	0.93
N_{measd} [$R_{(int)}$]	11128[0.0476]	14297[0.0403]	9838[0.0823]	11209 [0.1749]	15551[0.0779]	14831[0.2382]
R [$I > 2\sigma(I)$]	0.0687	0.0778	0.0725	0.1030	0.0846	0.1134
R_w [$I > 2\sigma(I)$]	0.1872	0.2251	0.2134	0.3099	0.2481	0.2276
GOF	0.867	1.066	0.922	0.958	1.094	1.012
	[Bu^{t}C5 · $Rb_2$2THF · H_2O]$_2$ · 1.5THF	**[Bu^{t}C5** · Cs_2 · 2THF · 2H_2O]$_2$ · 1.5THF	**[Bu^{t}C5** · Li_3 · 3THF · H_2O]$_2$ · 2CH_2Cl_2	**[Bu^{t}C5** · Li_3 · 2THF · 2H_2O]$_2$ · 2THF	**[Bu^{t}C5** · Na_3 · 2THF]$_2$ · 3.5THF	**[Bu^{t}C5** · Na_3 · THF · 4DMSO] · 2THF
Formula	C_{132} $H_{184}O_{17.5}$ Rb_4	$C_{132}H_{188}Cs_4$ $O_{19.5}$	$C_{136}H_{190}Cl_4Li_6O_{18}$	$C_{134}H_{190}Li_6$ O_{20}	$C_{140}H_{194}Na_6O_{17.5}$	$C_{75}H_{115}Na_3O_{12}S_4$
Formula weight	2392.73	2618.51	2296.41	2162.58	2294.96	1405.88
Crystal system	Monoclinic	Monoclinic	Monoclinic	Triclinic	Triclinic	Monoclinic
Space group	$C2/c$	$C2/c$	$P2_1/c$	$P\bar{1}$	$P\bar{1}$	$C2/m$
T (K)	213(2)	223(2)	213(2)	213(2)	213(2)	213(2)
a (Å)	38.854(2)	39.5795(16)	17.7408(16)	12.5244(10)	18.031(6)	25.352(8)
b (Å)	16.1785(9)	16.0732(6)	24.315(2)	15.3805(14)	18.856(6)	18.019(5)
c (Å)	21.4390(12)	21.5063(9)	17.1428(17)	18.6388(16)	23.754(7)	20.226(6)
α (°)	90	90	90	99.127(2)	108.640(5)	90
β (°)	91.0460(10)	91.1230(10)	117.360(2)	96.553(2)	93.571(6)	119.548(4)
γ (°)	90	90	90	103.382(2)	111.761(5)	90
V (A^3)	13474.2(13)	13679.0(9)	6567.7(11)	3405.9(5)	6956(4)	8038(4)
Z	4	4	2	1	2	4
d_{calcd} (g cm^{-3})	1.122	1.213	1.159	1.050	0.975	1.162
μ (mm^{-1})	1.498	1.113	0.152	0.068	0.078	0.189
Reflections collected	22368	50002	18144	8451	43727	30637
T_{min}/T_{max}	0.765	0.853	0.970	0.987	0.985	0.994
N_{measd} [$R_{(int)}$]	13404[0.0559]	16071[0.0634]	10894[0.0934]	8376[0.0324]	24370[0.0404]	9723[0.0764]
R [$I > 2\sigma(I)$]	0.0595	0.0524	0.0795	0.0824	0.1038	0.1082
R_w [I>2$\sigma(I)$]	0.1439	0.1534	0.1855	0.2609	0.2929	0.3249
GOF	0.927	1.021	0.903	1.109	1.110	1.205

3.5.5.2. Sodium. The crystal structure of compound **Bu^{t}C5** · Na · S (S = THF or MeCN) is shown in Fig. 9. The Na1 and Na1A atoms in **Bu^{t}C5** · Na · THF display a distorted trigonal bipyramidal geometry. Each Na atom is coordinated to three aryloxides from the first calixarene ring, one aryloxide from the second ring (O4 or O4A), and a THF molecule. In addition, a weak Na–O3 interaction is observed with a distance of 2.973(2) Å. For **Bu^{t}C5** · Na · MeCN, the Na1 and Na1A are coordinated to four oxygen atoms from the first calixarene ring, a single oxygen (O4 or O4A) from the second ring, and a strongly bonded MeCN [Na1–N1, 2.372(5) Å] to give a pseudo-octahedral geometry. Similar Na geometries are observed in **Bu^{t}C4** · Na monoanions [29,31] and some sodium atoms in the core cluster of Floriani's **Bu^{t}C4** · Na_4 [45]. All the Na–O bond distances fall within normal ranges (see Table 2). The structures **Bu^{t}C5** · Na · S exhibit a four membered $Na_2(\mu\text{-}O)_2$ core with the two sodium atoms bridged by O4 and O4A. The $Na_2(\mu\text{-}O)_2$ core forms a rectangle with Na1–O4 and Na1–O4A distances of 2.696(3) and 2.407(3) Å, respectively, when S = MeCN, and distances of 2.461(2) and 2.681(2) Å, respectively when S = THF.

The dimer **Bu^{t}C5** · Na_3 · 2THF (Fig. 11) shows an architecture similar to that of the lithium trianion (Fig. 9). Two oxo-bridged tetra-coordinated sodium atoms (Na1 and Na1A) link the two calixarene rings and the cone conformation is observed. A four membered $Na_2(\mu O)_2$ core is observed with Na–O distances of 2.298(3) and 2.346(3) Å. The O–Na–O and Na–O–Na angles are 96.49(10) and 83.51(10)°, respectively. The main distinction of the sodium trianion structure is the fact that the third sodium atom (Na3) apparently has a higher O-bridging affinity than the lithium. The Na3 cation is located inside the cavity (like Li3) but it is also bonded to O1 and O4 from the calixarene ring. This coordination environment for Na3 is similar to that observed in the tetraanion **Bu^{t}C4** · Na_4 reported by Floriani and coworkers [45]. The Na–C interactions range between 2.739(4) and 3.031(4) Å. All sodium atoms in **Bu^{t}C5** · Na_3 · 2THF are four-coordinate with geometry close to tetrahedral.

The crystal structure of **Bu^{t}C5** · Na_3 · THF · 4DMSO (Fig. 8) includes one sodium atom (Na1) centered between the five phenolic oxygens of the calixarene, one THF, and one DMSO molecule in a geometry close to pentagonal bipyramidal. The other two sodium atoms (Na2 and Na3) are coordinated to four DMSO molecules on one side, and three calixarene phenolic oxygen atoms on the other. The calixarene oxygen O3 and DMSO oxygen O7 triply bridge the 3 sodium atoms in the core structure with Na–OAr distances of 2.293(3)–2.532(4) Å. There is just one possible weak M–C interaction, Na1–C29 [2.979(6) Å], allowing the calixarene ring to retain the cone conformation. This particular example points out the importance of the solvate in the solid structure of the calixanions, because the terminal DMSO molecules on Na2 and Na3 atoms block the possible formation of a dimeric structure.

3.5.5.3. Potassium. The overall structure of **Bu^{t}C5** · K_2 · 4DMSO can be viewed as a dimer (Fig. 12) containing two different types of potassium atoms. The asymmetric unit shows K2 and K2A atoms occupying the central position of the lower rim of the calixarene ligands despite the fact that the oxygen atom in ring E does not participate in binding. The K1 and K1A atoms are coordinated to O4 and O5 from different calixarene ligands and to O6, O7, and O8 from three different DMSO molecules (DMSO containing O6 omitted for clarity). The calixarene oxygen atoms O4 and O5 μ^2-bridge K2 with K1 and K1A, respectively, while O5A and O4A μ^2-bridge K2A with K1 and K1A, respectively. The overall K_4O_8 core structure of **Bu^{t}C5** · K_2 · 4DMSO contains a central $K_4(\mu\text{-}O)_4$ eight membered ring (formed by K1, K2, K1A, K2A, O4, O5, O5A, and O4A) that adopts a pseudo chair conformation, with K–O distances in the range of 2.654(8)–2.823(8) Å. A DMSO molecule is in the calixarene cavity.

3.5.5.4. Rubidium and cesium. These metals display four-, seven- and eight-coordinate geometries in their calixarene complexes, as is typical for their aryloxide complexes [42]. π-Cation interaction becomes progressively more important for these metals, causing the change in the ring conformation to flattened cone.

In the crystal structure of **Bu^{t}C5** · Rb · THF (Fig. 6), the Rb atom is coordinated to three oxygen atoms of the calixarene ring and participates in η^2 and η^4 π-arene interactions. A special feature of the structure is the bonding of one THF molecule to the Rb atom through the hydrophobic cavity of the calixarene, thus combining coordination to the metal ion and inclusion in the calixarene, in a similar way to that reported for the coordination of pyridine N-oxide in $Na_8[Tb_4(C_5H_5NO)_4(H_2O)_{18}L'_4]$ (L′ = *p*-sulfonatocalix[5]arene) [46]. The **^{t}BuC5** · Cs · THF (Fig. 7) monomer shows the same architecture as the Rb one with the metal being coordinated to three oxygen atoms, but in this case the π-arene interactions increase to η^5, η^5.

In the X-ray structure of [**Bu^{t}C5** · Rb_2 · 2THF·H_2O]$_2$ (Fig. 13) two types of rubidium atoms are present in the asymmetric unit. Rb2 and Rb2A (by symmetry) bind *exo* and bridge the two **Bu^{t}C5** cones through Rb–O contacts. Rb2 and Rb2A atoms are coordinated to four oxygens from the first calixarene unit, one oxygen atom (O5 or O5A) from the second calixarene, one THF solvate and one water molecule to give an overall heptacoordination with geometry close to capped octahedral. The other type of Rb atom (Rb1 and Rb1A) binds *endo* within the calixarene cone with contacts to the phenyl rings by π-cation interactions. Rb1 and Rb1A are coordinated to three oxygens from the calixarene ligand, and the hydrophobic cavity is large enough to allow the inclusion of a THF coordinated to Rb1. The core structure located in the lower rim could be described as a $Rb_2(\mu\text{-}O)_2$ four membered ring with Rb2–O5 and Rb2–O5A distances of 3.294(3) and 2.820(3) Å, and O–Rb–O and Rb–O–Rb angles of 79.73(9) and 91.31(8)°. The $Rb_2(\mu\text{-}O)_2$ ring deviates from planarity with a torsion angle of 34.12(9)°. Due to the strong π-arene interactions of Rb1 and Rb1A the calixarene ligands show a flattened cone conformation with the 1,3 phenyl groups essentially oriented in the same direction.

[**Bu^{t}C5** · Cs_2 · 2THF · $2H_2O$]$_2$ (Fig. 14) shows roughly the same architecture as [**Bu^{t}C5** · Rb_2 · 2THF · H_2O]$_2$, being a dimeric structure containing octa-coordinated *exo* cesium atoms (Cs2 and Cs2A) and tetra-coordinated (not including π coordination) *endo* cesium atoms, Cs1 and Cs1A. As expected, the endo cesium atoms exhibit a stronger π-cation interaction with the phenyl rings (there are M–C interactions with three of the arene rings) in comparison with the smaller cations mentioned earlier. Because of the bigger size of Cs in comparison to Rb, one THF and two water molecules are coordinated to Cs2 and Cs2A atoms in the lower rim.

3.5.6. X-ray structure information

See Table 3.

4. Conclusion

We have reported the high-yield synthesis and complete characterization for a comprehensive series of *p-tert*-butylcalix[5]arene mono-, di-, tri-, and pentaanions. The synthesis consists of the simple addition of base to the parent calixarene, but the choices of the base, stoichiometry, and solvent are very important.

NMR and X-ray structural studies show that the complexes with lithium and sodium are in their cone conformations and the structures with potassium, rubidium, and cesium contain the flattened cone conformation. The degree of flexibility of the ring depends

mainly on the nature of the metal and the deprotonation level of the complex.

We have illustrated the variety of structural types available to alkali metal salts of *p-tert*-butylcalix[5]arene in the solid state. These include monomeric and dimeric units. Bulky *tert*-butyl groups in the upper rim of the **Bu^{t}C5** appear to block polymer formation in the solid state. Alkali metal atoms were found to bind the calixarene ring in the *endo* and *exo* positions. Alkali metal cation-π interactions can be observed for most alkali metals, and these interactions become progressively more important as the size of the alkali metal increases.

5. Experimental

5.1. General information

Unless otherwise noted, all manipulations were carried out in a nitrogen filled glove-box or using standard Schlenk techniques. Starting materials were obtained from commercial suppliers and used without further purification.

para-tert-Butylcalix[5]arene was prepared by the literature procedure [47] and was dried at 110 °C at least 24 h under vacuum before use. Tetrahydrofuran was freshly distilled from Na/benzophenone. Methanol was passed through a column of dried 4 Å molecular sieves, kept over 4 Å sieves for 15 days, then the solvent was distilled and stored over 4 Å molecular sieves. Benzene was dried by refluxing over Na/benzophenone and stored over 4 Å molecular sieves. Other anhydrous solvents were purchased from Aldrich and stored over molecular sieves under nitrogen before using. Deuterated benzene, dimethyl sulfoxide, and chloroform were dried over CaH_2. The melting points of all the compounds were taken in capillary tubes on a Mel-temp apparatus (Laboratory devices, Cambridge, MA) using a 500 °C thermometer calibrated against a thermocouple. ^{1}H NMR and ^{13}C spectra were recorded at room temperature on a Varian XL-300 spectrometer at 300 and 75 MHz, respectively. Analytical samples were dried under vacuum for at least 24 h (for M = Li, Na, K salts only). Microanalyses were performed by Atlantic Microlab, Inc, Norcross, GA. IR and UV–Vis spectra were obtained with an infinity Gold™ FTIR spectrometer and Agilent 8453 spectrophotometer, respectively. Filtrations used a medium sintered glass filter. X-ray data for [**Bu^{t}C5** · Na_2 · 2THF]$_2$ · 3.5THF and [**Bu^{t}C5** · K_2 · 4DMSO]$_2$ · 8DMSO were collected on a Bruker SMART APEX CCD diffractometer at low temperature using Mo Kα radiation. All other X-ray diffraction experiments were performed on a Bruker SMART 1000 CCD detector at variable low temperature using Mo Kα radiation. In some cases the positions of the phenolic hydrogens have been located in the crystal structures, while in other cases the positions may be inferred by comparison of O–O distances and/or M–O bond lengths. In most cases the crystals for X-ray diffraction included solvents of crystallization, as shown in Table 3. For analytical samples solvents were removed as much as conveniently possible.

5.2. Monoanion syntheses

Bu^{t}C5 · Na: *Method A*: $NaOC(CH_3)_3$ (0.0490 g, 0.509 mmol) in THF (5 mL) was added dropwise to a solution of **Bu^{t}C5** (0.412 g, 0.508 mmol) in THF (10 mL). The colorless solution was allowed to stir for 24 h at room temperature with no visible change. The solvent was removed by vacuum yielding a white powder. The powder was washed with pentane (5 mL) and allowed to settle. The remaining pentane was removed using a pipette. This washing procedure was repeated. Recrystallization of the powder was performed either by pentane diffusion into its THF solution or by slow evaporation in air of a concentrated acetonitrile solution to give colorless crystals of **Bu^{t}C5** · Na (0.349 g, 83% yield). Single crystals were obtained from the slow evaporation in air of a concentrated THF/acetonitrile/pentane (2:1:1 ratio) solution of the product.

Method B: A suspension of NaH (0.0120 g, 0.510 mmol) in THF (5 mL) was added to a solution of **Bu^{t}C5** (0.412 g, 0.508 mmol) in THF (10 mL). The white suspension was allowed to stir for 24 h at room temperature. The mixture was filtered and the remaining solid NaH was removed. The filtrate was dried under reduced pressure yielding a white-yellowish mixture (mixture of **Bu^{t}C5** and **Bu^{t}C5** · Na). This crude material was washed twice with pentane (5 mL portions). Filtration and vacuum drying for 2 h at room temperature led to the product as a white powder. The solid was recrystallized either by slow evaporation of solvent (THF) or by pentane diffusion in a THF solution yielding colorless crystals of **Bu^{t}C5** · Na (0.346 g, 81% yield).

Method C: Under air, a suspension of Na_2CO_3 (0.0540 g, 0.510 mmol) in MeCN or THF (10 mL) was added to a solution of **Bu^{t}C5** (0.412 g, 0.508 mmol) in MeCN or THF (20 mL). The white suspension was refluxed under nitrogen for 24 h. The mixture was filtered and the remaining solid Na_2CO_3 was removed. The filtrate was dried under reduced pressure yielding a white-yellowish mixture (mixture of **Bu^{t}C5** and **Bu^{t}C5** · Na). This crude material was washed twice with pentane (5 mL portions). Filtration and vacuum drying for 2 h at room temperature led to the product as a white powder. The solid was recrystallized either by slow evaporation of solvent (THF) or by pentane diffusion in a THF solution yielding colorless crystals of **Bu^{t}C5** · Na (0.306 g, 72% yield). Single crystals were obtained by the slow evaporation in air of a concentrated acetonitrile solution of the product. M.p. 444–446 °C; ^{1}H NMR ($CDCl_3$, TMS): δ = 1.23 (s, 45H, C(CH_3)$_3$), 3.47 (b, 5H, ArCH_2Ar), 4.37 (b, 5H, ArCH_2Ar), 7.18 ppm (s, 10H, Ar*H*). OH peaks were too broad to be observed at rt; ^{13}C NMR ($CDCl_3$, TMS): δ = 31.7 (C(CH_3)$_3$), 31.9 (*C*(CH_3)$_3$), 34.1 (ArCH_2Ar), 125.9, 127.4, 143.1, 149.2 ppm (aromatic carbons); IR (KBr): ν = 3431m (OH), 3306m (OH), 3052w, 2961vs, 2911w, 2868w, 1607w, 1483vs, 1389w, 1362m, 1294m, 1248w, 1204s, 1196w, 874m, 818 cm^{-1} (w); UV–Vis (THF) λ_{max}/nm (ε/dm^3 mol^{-1} cm^{-1}): 286 (7.84×10^4), 280 (7.83×10^3), 241 (4.43×10^3). Elemental Anal. Calc. for $C_{55}H_{69}O_5Na \cdot C_2H_3N$: C, 78.30; H, 8.33. Found: C, 78.49; H, 8.56%.

Bu^{t}C5 · K: *Method A*: A solution of $KOC(CH_3)_3$ (0.0571 g, 0.517 mmol) in THF (5 mL) was added dropwise to a solution of **Bu^{t}C5** (0.412 g, 0.508 mmol) in THF (10 mL) and the resulting clear solution was allowed to stir for 24 h at rt. The solvent of the final colorless solution was removed by vacuum yielding a white-yellowish powder. This crude material was washed twice with pentane (5 mL portions). Filtration and vacuum drying for 2 h at room temperature led to the product as a white powder. The solid was recrystallized by either pentane diffusion into its THF solution or by slow evaporation in air of an acetonitrile solution to give colorless crystals of **Bu^{t}C5** · K (0.369 g, 86% yield).

Method B: Under air, a suspension of K_2CO_3 (0.0591 g, 0.519 mmol) in MeCN or THF (10 mL) was added to a solution of **Bu^{t}C5** (0.412 g, 0.508 mmol) in MeCN or THF (20 mL). The white suspension was refluxed under nitrogen for 24 h. At the end of the reaction the white mixture was filtered and the remaining solid K_2CO_3 was removed. The filtrate was dried under reduced pressure yielding a white-yellowish mixture (mixture of **Bu^{t}C5** and **Bu^{t}C5** · K). This crude material was washed twice with pentane (5 mL portions). Filtration and vacuum drying led to the product as a white powder. The solid was recrystallized either by slow evaporation of a THF solution or by pentane diffusion in a THF solution yielding white crystalline needles of **Bu^{t}C5** · K (0.357 g, 82% yield). Single crystals were obtained after two weeks by diffusion of pentane in a THF/DMSO (5:1) solution of the product. M.p. 303–305 °C; ^{1}H NMR ($CDCl_3$, TMS): δ = 1.21 (s, 45H, C(CH_3)$_3$), 3.86 (b, 10H, ArCH_2Ar), 7.11 (s, 10H, Ar*H*),

8.66 ppm (b, 4H, O*H*); ^{13}C NMR ($CDCl_3$, TMS): δ = 31.6 (C(CH_3)$_3$), 32.7 (*C*(CH_3)$_3$), 33.8 (ArCH_2Ar), 125.6, 128.7, 140.9, 151.9 ppm (aromatic carbons); IR (KBr): ν = 3298s (OH), 3052w, 2961vs, 2911w, 2869w, 1599w, 1482s, 1393w, 1362m, 1292m, 1236w, 1199s, 1117m, 881w, 819 cm^{-1} (w); UV–Vis (THF) λ_{max}/nm (ε/dm^3 mol^{-1} cm^{-1}): 287 (4.152×10^3), 241 (4.255×10^3). Elemental Anal. Calc. for $C_{55}H_{69}O_5K \cdot C_2H_3N$: C, 76.86; H, 8.15. Found: C, 76.47; H, 8.13%.

Bu^{t}C5 · Rb*:* Under air, dry methanol (5 mL) was added to a solution of **Bu^{t}C5** (0.202 g, 0.250 mmol) and $RbOH \cdot H_2O$ (0.0301 g, 0.250 mmol) in benzene (25 mL). The reaction mixture was refluxed 12 h under N_2 with a Dean-Stark condenser. All volatiles were removed under vacuum and a white solid was obtained. The product was purified by diffusion of pentane into a concentrated THF solution yielding colorless crystals of **Bu^{t}C5** · Rb (0.198 g, 86% yield). The same procedure can be done with Rb_2CO_3 (0.0304 g, 0.125 mmol) to produce the same product. M.p. 205 °C (decomp); ^{1}H NMR ($CDCl_3$, TMS): δ = 1.23 (s, 45H, C(C*H*$_3$)$_3$), 3.86 (b, 10H, ArC*H*$_2$Ar), 7.12 ppm (s, 10H, Ar*H*). The OH peaks were not observed at rt; ^{13}C NMR ($CDCl_3$, TMS): δ = 31.5 (C(*C*H$_3$)$_3$), 32.4 (*C*(CH$_3$)$_3$), 33.9 (ArCH$_2$Ar), 125.6, 128.2, 142.0, 150.6 ppm (aromatic carbons); IR (KBr): ν = 3426s (OH), 3309sh, 2960s, 2906m, 2868m, 1610w, 1483s, 1363m, 1294m, 1260m, 1204s, 1101m, 1020m, 878m, 803 cm^{-1} (m); UV–Vis (THF) λ_{max}/nm (ε/dm^3 mol^{-1} cm^{-1}): 286 (4.218×10^4), 240 (1.271×10^3). Elemental Anal. Calc. for $C_{55}H_{69}O_5Rb \cdot C_4H_8O$: C, 73.21; H, 8.03. Found: C, 72.94; H, 8.06%.

Bu^{t}C5 · Cs: The same procedure as the one performed for **Bu^{t}C5** · Rb was followed, using **Bu^{t}C5** (0.203 g, 0.250 mmol) and $CsOH \cdot H_2O$ (0.0421 g, 0.251 mmol). The product was purified by diffusion of pentane into a concentrated THF solution to obtain **Bu^{t}C5** · Cs as block colorless crystals (0.202 g, 86% yield). The same procedure can be done with Cs_2CO_3 (0.0418 g, 0.125 mmol) to produce the same product. M.p. 225 °C (decomp); ^{1}H NMR ($CDCl_3$, TMS): δ = 1.22 (s, 45H, C(C*H*$_3$)$_3$), 3.46 (b, 5H, ArC*H*$_2$Ar), 4.21 (b, 5H, ArC*H*$_2$Ar), 7.10 (s, 10H, Ar*H*), 8.75 ppm (b, 4H, O*H*); ^{13}C NMR ($CDCl_3$, TMS): δ = 31.6 (C(*C*H$_3$)$_3$), 32.3 (*C*(CH$_3$)$_3$), 33.8 (ArCH$_2$Ar), 125.6, 128.2, 141.9, 151.1 ppm (aromatic carbons); IR (KBr): ν = 3409s (OH), 2960s, 2904m, 2866m, 1612w, 1483s, 1363m, 1292m, 1257m, 1205s, 1118w, 1018w, 879w, 818 cm^{-1} (w); UV–Vis (THF) λ_{max}/nm (ε/dm^3 mol^{-1} cm^{-1}): 285 (1.966×10^4), 241 (1.190×10^4). Elemental Anal. Calc. for $C_{55}H_{69}O_5Cs$: C, 69.58; H, 7.89. Found: C, 69.23; H, 7.90%.

5.3. Dianion synthesis

Bu^{t}C5 · Na_2: $NaOC(CH_3)_3$ (0.0980 g, 1.01 mmol) in THF (5 mL) was added dropwise to a solution of **Bu^{t}C5** (0.412 g, 0.508 mmol) in THF (15 mL). The light yellow solution was allowed to stir at rt for 24 h, then was dried under vacuum yielding a white solid. Hexane (10 mL) was added to the solid and the mixture was stirred for 15 min. Pure **Bu^{t}C5** · Na_2 was obtained as a white powder after filtration (0.400 g, 92% yield). M.p. 450 °C (decomp); ^{1}H NMR ([D_6]DMSO, TMS): δ = 1.16 (s, 45H, C(C*H*$_3$)$_3$), 3.09 (b, 5H, ArC*H*$_2$ Ar), 4.22 (b, 5H, ArC*H*$_2$Ar), 6.96 (s, 10H, Ar*H*), 15.38 ppm (b, 3H, O*H*); ^{1}H NMR ($CDCl_3$, TMS): δ = 1.22 (s, 45H, C(C*H*$_3$)$_3$), 2.85 (b, 5H, ArC*H*$_2$Ar), 4.03 (s, 5H, ArC*H*$_2$Ar), 6.97 ppm (s, 10H, Ar*H*). OH peaks were too broad to be observed at rt.; ^{13}C NMR ([D_6]DMSO, TMS): δ = 3 (C(*C*H$_3$)$_3$), 33.3 (*C*(CH$_3$)$_3$), 34.0 (ArCH$_2$Ar), 124.9, 127.9, 137.8, 154.7 ppm (aromatic carbons); IR (KBr): ν = 3415m (OH), 3048w, 2961vs, 2904s, 2863s, 2356w, 1607w, 1482vs, 1393m, 1362s, 1295s, 1240m, 1204vs, 115w, 874m, 817m, 794 cm^{-1} (m); UV–Vis (THF) λ_{max}/nm (ε/dm^3 mol^{-1} cm^{-1}): 242 (1.682×10^4), 286 (1.586×10^4). Elemental Anal. Calc. for $C_{55}H_{68}O_5Na_2 \cdot 2.5(C_4H_8O)$: C, 75.40; H, 8.57. Found: C, 75.09; H, 8.76.

Bu^{t}C5 · K_2: A solution of $KOC(CH_3)_3$ (0.114 g, 1.01 mmol) in THF (5 mL) was added dropwise to a solution of **Bu^{t}C5** (0.412 g, 0.508 mmol) in THF (15 mL). The light yellow solution was allowed to stir at rt for 24 h, then was dried under vacuum yielding a white solid. Hexane (10 mL) was added to the solid and the mixture was stirred for 15 min. Pure **Bu^{t}C5** · K_2 was obtained as a white powder after filtration (0.434 g, 96% yield). Crystals suitable for X-ray analysis were obtained by slow evaporation of a concentrated THF/DMSO (10:1 ratio) solution of **Bu^{t}C5** · K_2. M.p. 353–355 °C; ^{1}H NMR ([D_6]DMSO, TMS): δ = 1.16 (s, 45H, C(C*H*$_3$)$_3$), 3.06 (b, 5H, ArC*H*$_2$Ar), 4.27 (b, 5H, ArC*H*$_2$Ar), 6.94 (s, 10H, Ar*H*), 15.15 ppm (b, 3H, O*H*); ^{1}H NMR ($CDCl_3$, TMS): δ = 1.20 (s, 45H, C(C*H*$_3$)$_3$), 3.77 (b, 10H, ArC*H*$_2$Ar), 7.06 ppm (s, 10H, Ar*H*). OH peaks were too broad to be observed at rt; ^{13}C NMR ([D_6]DMSO, TMS): δ = 32.4 (C(*C*H$_3$)$_3$), 33.2 (*C*(CH$_3$)$_3$), 33.9 (ArCH$_2$Ar), 124.9, 127.9, 136.9, 155.4 ppm (aromatic carbons); IR (KBr): ν = 3411m (OH), 3053w, 2960vs, 2094s, 2871m, 1603w, 1482vs, 1393w, 1362m, 1295m, 1232w, 1203s, 1124w, 874w, 818 cm^{-1} (w); UV–Vis (THF) λ_{max}/nm (ε/dm^3 mol^{-1} cm^{-1}): 277 (8.154×10^5), 287 (8.90×10^5). Elemental Anal. Calc. for $C_{55}H_{68}O_5K_2 \cdot C_2H_6SO$: C, 70.90; H, 7.73. Found: C, 71.09; H, 7.76%.

Bu^{t}C5 · Rb_2: Under air, dry methanol (5 mL) was added to a solution of **Bu^{t}C5** (0.205 g, 0.253 mmol) and Rb_2CO_3 (0.0607 g, 0.250 mmol) in benzene (25 mL). The reaction mixture was refluxed 12 h under N_2 with a Dean-Stark condenser. All volatiles were removed under vacuum and a white solid was obtained. The product was purified by diffusion of pentane into a concentrated THF solution yielding colorless crystals of **Bu^{t}C5** · Rb_2 (0.203 g, 83% yield). M.p. 235 °C (decomp); ^{1}H NMR ($CDCl_3$, TMS): δ = 1.20 (s, 45H, C(C*H*$_3$)$_3$), 3.86 (b, 10H, ArC*H*$_2$Ar), 7.07 (s, 10H, Ar*H*), 8.03 ppm (b, 3H, O*H*); ^{13}C ($CDCl_3$, TMS): δ = 31.6 (C(*C*H$_3$)$_3$), 33.1 (*C*(CH$_3$)$_3$), 33.8 (ArCH$_2$Ar), 125.5, 128.8, 140.7, 152.6 ppm (aromatic carbons). IR (KBr): ν = 3434s (OH), 2960s, 2908m, 2870m, 1633m, 1481s, 1362m, 1295m, 1261w, 1203m, 1107m, 1022m, 883w, 803 cm^{-1} (m); UV–Vis (THF) λ_{max}/nm (ε/dm^3 mol^{-1} cm^{-1}): 287 (2.167×10^4), 241 (1.817×10^4). Elemental Anal. Calc. for $C_{55}H_{68}O_5Rb \cdot C_4H_8O \cdot H_2O$: C, 66.20; H, 7.35. Found: C, 65.85; H, 7.32%.

Bu^{t}C5 · Cs_2*:* The same procedure as the one performed for **Bu^{t}C5** · Rb_2 was followed using **Bu^{t}C5** (0.207 g, 0.256 mmol) and Cs_2CO_3 (0.0834 g, 0.247 mmol). The product was purified by diffusion of pentane into a concentrated THF solution to obtain block colorless crystals of **Bu^{t}C5** · Cs_2 (0.215 g, 81% yield). M.p. 260 °C (decomp); ^{1}H NMR ($CDCl_3$, TMS): δ = 1.18 (s, 45H, C(C*H*$_3$)$_3$), 3.48 (b, 5H, ArC*H*$_2$Ar), 4.24 (b, 5H, ArC*H*$_2$Ar), 6.97 (s, 10H, Ar*H*), 13.49 ppm (b, 3H, O*H*); ^{13}C NMR ($CDCl_3$, TMS): δ = 31.0 (C(*C*H$_3$)$_3$), 33.2 (*C*(CH$_3$)$_3$), 33.8 (ArCH$_2$Ar), 125.4, 128.9, 139.9, 153.9 ppm (aromatic carbons); IR (KBr): ν = 3437s (OH), 2960s, 2908m, 2870m, 1633m, 1480s, 1362m, 1296m, 1261w, 1206m, 1099m, 1022m, 879w, 801 cm^{-1} (m); UV–Vis (THF) λ_{max}/nm (ε/dm^3 mol^{-1} cm^{-1}): 287 (1.766×10^4), 242 (1.885×10^4). Elemental Anal. Calc. for $C_{55}H_{68}O_5Cs_2 \cdot C_4H_8O$: C, 61.76; H, 6.68. Found: C, 61.95; H, 6.97%.

5.4. Trianion synthesis

Bu^{t}C5 · Li_3*: Method A*: Under air, a suspension of LiH (0.0130 g, 1.55 mmol) in THF (7 mL) was added to a solution of **Bu^{t}C5** (0.418 g, 0.515 mmol) in THF (10 mL). The white suspension was placed into a 100 mL round bottom flask, and then kept in reflux under nitrogen for 24 h. The final colorless solution was vacuum dried yielding a white solid. The solid was redissolved in THF (5 mL) and then recrystallized by the diffusion of pentane into the solution. After three days at rt colorless crystals appeared. The remaining solvent was removed and the crystals were dried under vacuum yielding **Bu^{t}C5** · Li_3 as a white solid (0.303 g, 71%).

Single crystals of the product were obtained by diffusion of dichloromethane into its THF solution.

The same procedure, but increasing the number of equivalents to 4 and 5 mmol of LiH, increased the yield of **Bu^{t}C5** · Li_3 to 82% (0.350 g) and 93% (0.396 g), respectively.

Method B: The same procedure of method A was performed using a solution of 0.0378 g (1.57 mmol) of LiOH (instead of LiH) in dry methanol (5 mL). The product was recrystallized from diffusion of pentane into THF solution to obtain 0.380 g (89% yield). In this case increasing the equivalents of LiOH to 4 and 5 increased the yields to 92 (0.392 g) and 94% (0.401 g), respectively.

Method C: A 2.0 M solution of *n*-BuLi in pentane (0.0931 g, 1.55 mmol) was added dropwise to a solution of **Bu^{t}C5** (0.420 g, 0.518 mmol) in THF (10 mL) to give a yellowish solution. The reaction mixture was allowed to stir for 24 h at rt. The solvent was removed under vacuum to give a yellowish solid. Pentane (5 mL) was added to the solid and allowed to stir for 5 min. The mixture was filtered to give 0.369 g of a white crystalline powder of pure **Bu^{t}C5** · Li_3 in 86% yield. Single crystals of the product were obtained by pentane diffusion into a concentrated THF solution of the product.

Method D: The same procedure as method C was performed using 1.58 mmol (0.126 g) of $LiOC(CH_3)_3$ (instead of *n*-BuLi) in THF (5 mL), to give **Bu^{t}C5** · Li_3 in 97% yield (0.413 g). M.p. 422–424 °C; ^{1}H NMR (C_6D_6, TMS): δ = 1.05 (s, 9H, C(C*H*$_3$)$_3$), 1.25 (s, 18H, C(C*H*$_3$)$_3$), 1.34 (s, 18H, C(C*H*$_3$)$_3$), 3.30 (d, 1H, *J* = 14 Hz, ArC*H*$_2$-Ar), 3.39 (d, 2H, *J* = 13 Hz, ArC*H*$_2$Ar), 3.72 (d, 2H, *J* = 14 Hz, ArC*H*$_2$-Ar), 4.18 (d, 1H, *J* = 14 Hz, ArC*H*$_2$Ar), 4.54 (d, 2H, *J* = 13 Hz, ArC*H*$_2$Ar), 5.73 (d, 2H, *J* = 14 Hz, ArC*H*$_2$Ar), 7.22 (b, 2H, Ar*H*), 7.32 (b, 2H, Ar*H*), 7.48 ppm (b, 6H, Ar*H*). OH peaks were not observed at rt; ^{13}C NMR (C_6D_6, TMS): δ = 25.0 (ArCH$_2$Ar), 31.3, 31.7, 31.8 (C(*C*H$_3$)$_3$), 32.5 (ArCH$_2$Ar), 33.5, 33.7, 33.8 (*C*(CH$_3$)$_3$), 36.4 (ArCH$_2$-Ar), 125.5, 125.8, 126.4, 126.7, 130.3, 130.5, 130.7, 138.6, 140.6, 152.8, 154.1, 158.7 ppm (aromatic carbons); IR (KBr): ν = 3519m (OH), 3423m (OH), 3049w, 2960vs, 2904m, 2871m, 1611w, 1482vs, 1446s, 1362m, 1291m, 1204w, 1112w, 877w, 817 cm^{-1} (w); UV–Vis (THF) λ_{max}/nm (ε/dm^3 mol^{-1} cm^{-1}): 289 (9.089×10^3). Elemental Anal. Calc. for $C_{55}H_{67}O_5Li_3 \cdot 4(C_4H_8O) \cdot CH_2Cl_2$: C, 71.93; H, 8.47. Found: C, 71.54; H, 8.27%.

Bu^{t}C5 · Na_3*:* A suspension of $NaOC(CH_3)_3$ (0.92 g, 2.02 mmol) in toluene (10 mL) was added dropwise to a solution of **Bu^{t}C5** (0.412 g, 0.508 mmol) in toluene (20 mL). The mixture was stirred at rt. After the first 2 h of stirring the starting yellowish mixture became a yellow-white mixture, and then it was allowed to stir for another 22 h. The yellowish mixture was dried under reduced pressure producing a yellowish solid. To the solid was added pentane (10 mL) and the mixture was stirred for 10 min. Filtration and vacuum drying of the solid led to the crude product as a white powder. Recrystallization of the powder was performed either by slow evaporation of solvent (THF) or by pentane diffusion into a THF solution yielding 0.423 g of **Bu^{t}C5** · Na_3 (93% yield). The slow evaporation of a concentrated THF/DMSO (10:1) solution of the product gave block colorless single crystals suitable for X-ray analysis. M.p. 434–436 °C; ^{1}H NMR (C_6D_6, TMS): δ = 1.33 (s, 9H, C(C*H*$_3$)$_3$), 1.39 (s, 18H, C(C*H*$_3$)$_3$), 1.49 (s, 18H, C(C*H*$_3$)$_3$), 3.27 (d, 1H, *J* = 12 Hz, ArC*H*$_2$Ar), 3.35 (d, 1H, *J* = 12 Hz, ArCH$_2$Ar), 3.44 (d, 2H, *J* = 13 Hz, ArC*H*$_2$Ar), 3.67 (d, 2H, *J* = 14 Hz, ArC*H*$_2$Ar), 4.27 (d, 2H, *J* = 14 Hz, ArC*H*$_2$Ar), 4.37 (d, 2H, *J* = 13 Hz, ArC*H*$_2$Ar), 7.33 (s, 2H, Ar*H*), 7.38 (s, 2H, Ar*H*), 7.53 (s, 2H, Ar*H*), 7.60 (s, 2H, Ar*H*), 7.67 ppm (s, 2H, Ar*H*); OH peaks were not observed at rt. ^{13}C NMR could not be obtained due to insufficient solubility; IR (KBr): ν = 3542m (OH), 3352m (OH), 3054w, 2960vs, 2906s, 2867s, 1609w, 1481vs, 1391m, 1363s, 1293s, 1206s, 1164m, 1002m, 904m, 885m, 819 cm^{-1} (m); UV–Vis (THF) λ_{max}/nm (ε/dm^3 mol^{-1} cm^{-1}): 298 (1.267×10^4). Elemental Anal. Calc. for $C_{55}H_{67}O_5Na_3 \cdot 3(C_2H_6SO)$: C, 65.92; H, 7.71. Found: C, 66.17; H, 7.47%.

Bu^{t}C5 · K_3*:* $KOC(CH_3)_3$ (0.173 g, 1.54 mmol) in THF (10 mL) was added dropwise to a solution of **Bu^{t}C5** (0.416 g, 0.509 mmol) in THF (20 mL). The colorless solution was stirred at rt for 24 h. The final yellowish solution was dried under reduced pressure producing a yellowish solid. The solid was redissolved in THF (5 mL), and hexane diffusion caused the precipitation of white solid. Filtration and vacuum drying of the solid led to the crude product as a white powder. The powder was washed twice with pentane (5 mL) to give 0.458 g of pure **Bu^{t}C5** · K_3 (97% yield). Single colorless crystals were obtained after two weeks by the slow evaporation of a concentrated THF/DMSO (5:1 ratio) solution of the product. M.p. 383–384 °C; ^{1}H NMR (C_6D_6, TMS): δ = 1.51 (s, 45H, C(C*H*$_3$)$_3$), 3.45 (b, 5H, ArC*H*$_2$Ar), 4.29 (b, 5H, ArC*H*$_2$Ar), 7.69 ppm (s, 10H, Ar*H*). No OH peaks were observed at rt; ^{13}C NMR (C_6D_6, TMS): δ = 31.9 (C(*C*H$_3$)$_3$), 33.9 (*C*(CH$_3$)$_3$), 40.3 (ArCH$_2$Ar), 125.5, 129.2, 140.0, 153.6 ppm (aromatic carbons). IR (KBr): ν = 3413m (OH), 2858vs, 2906s, 2868m, 2360m, 1642m, 1477vs, 1401s, 1362m, 1299s, 1202m, 1123w, 1030s, 953m, 881m, 815 cm^{-1} (m). UV–Vis (THF) λ_{max}/nm (ε/dm^3 mol^{-1} cm^{-1}): 307 (9.041×10^3). Elemental Anal. Calc. for $C_{55}H_{67}O_5K_3$: C, 71.38; H, 7.30. Found: C, 71.00; H, 7.58%.

5.5. Pentaanion synthesis

Bu^{t}C5 · Li_5*:* A solution of $LiOC(CH_3)_3$ (0.206 g, 2.58 mmol) in THF (5 mL) was added to a solution of **Bu^{t}C5** (0.418 g, 0.515 mmol) in THF (15 mL). The yellow solution obtained was stirred at rt for 24 h. The final yellow-orange solution was vacuum dried yielding a white-yellow solid. The solid was washed twice with hexane (5 mL portions) and filtered. The white solid obtained gave 0.398 g of **Bu^{t}C5** · Li_5 (77% yield).

Method B: A 2 M solution of *n*-BuLi in pentane (0.0840 g, 1.40 mmol) was added dropwise to a solution of **Bu^{t}C5** (0.214 g, 0.254 mmol) in THF (10 mL) and the reaction mixture was allowed to stir for 24 h at rt. The solvent was vacuum evaporated yielding a yellowish powder. Pure **Bu^{t}C5** · Li_5 (0.168 g, 78%) was obtained after washing the crude material twice with pentane (5 mL portions). Single crystals could be obtained from the slow evaporation of a concentrated THF: DMSO (10:1) solution of product, but the crystals did not diffract well. M.p. 436 °C; ^{1}H NMR ([*D*$_6$]DMSO, TMS): δ = 1.07 (s, 45H, C(CH$_3$)$_3$), 2.69 (d, 5H, *J* = 12 Hz, ArC*H*$_2$Ar), 4.30 (d, 5H, *J* = 13 Hz, ArC*H*$_2$Ar), 6.94 ppm (s, 10H, Ar*H*); ^{1}H NMR (C_6D_6, TMS): δ = 1.41 (s, 45H, C(C*H*$_3$)$_3$), 3.57 (b, 5H, ArC*H*$_2$ Ar), 4.02 (b, 5H, ArC*H*$_2$ Ar), 7.47 ppm (s, 10H, Ar*H*); ^{13}C NMR (C_6D_6): δ = 25.3 (C(CH$_3$)$_3$), 31.9 (*C*(CH$_3$)$_3$), 33.7 (ArCH$_2$Ar), 125.6, 129.7, 137.9, 157.7 ppm (aromatic carbons). IR (KBr): ν = 3048w, 2959vs, 2904s, 2867s, 1606w, 1481vs, 1456s, 1392s, 1361s, 1295vs, 1204m, 1044w, 906w, 875w, 820m, 804 cm^{-1} (m). UV–Vis (THF) λ_{max}/nm (ε/dm^3 mol^{-1} cm^{-1}): 283 (3.95×10^4). Elemental Anal. Calc. for $C_{55}H_{65}0_5Li_5 \cdot 3(C_2H_6SO)$: C, 68.14; H, 7.78. Found: C, 67.94; H, 7.91%.

Bu^{t}C5 · Na_5*:* A suspension of $NaOC(CH_3)_3$ (0.247 g, 2.58 mmol) in toluene (5 mL) was added to a solution of **Bu^{t}C5** (0.418 g, 0.515 mmol) in toluene (15 mL). The white cloudy solution obtained was stirred at rt for 24 h. The final white mixture was vacuum dried yielding a white-yellowish solid. The solid was washed twice with hexane (5 mL portions) and filtered. The white solid obtained gave 0.435 g of **Bu^{t}C5** · Na_5 (91% yield). M.p. 466 °C (decomp); ^{1}H NMR ([D$_6$]DMSO, TMS): δ = 1.07 (s, 45H, C(C*H*$_3$)$_3$), 2.69 (d, 5H, *J* = 13 Hz, ArC*H*$_2$Ar), 4.14 (d, 5H, *J* = 13 Hz, ArC*H*$_2$Ar), 6.79 ppm (s, 10H, *ArH*); ^{13}C NMR could not be obtained due to insufficient solubility; IR (KBr): ν = 3042w, 2959vs, 2905s, 2867s, 1557w, 1478vs, 1392s, 1361s, 1294vs, 1237w, 1202m, 882 cm^{-1} (w). UV–Vis (THF) λ_{max}/nm (ε/dm^3 mol^{-1} cm^{-1}): 287 (2.511×10^4). Elemental Anal. Calc. for $C_{55}H_{67}O_5Na_5$: C, 71.72; H, 7.11. Found: C, 71.43; H, 7.43%.

Bu^{t}C5 · K_5: The same procedure as the one performed for **Bu^{t}C5** · Na_5 was followed, using **Bu^{t}C5** (0.418 g, 0.515 mmol) and $KOC(CH_3)_3$ (0.291 g, 2.59 mmol). Filtration gave 0.451 g of **Bu^{t}C5** · K_5 as a white crystalline powder (87% yield). M.p. 465 °C; ^{1}H NMR ([D_6]DMSO, TMS): δ = 0.97 (s, 45H, C(CH_3)$_3$), 2.51 (d, 5H, J = 16 Hz, ArCH_2Ar), 4.18 (d, 5H, J = 13 Hz, ArCH_2Ar), 6.55 ppm (s, 10H, *ArH*). ^{13}C NMR ([D_6]DMSO, TMS) δ = 31.9 (C(CH_3)$_3$), 32.7 (C(CH_3)$_3$), 33.5 (ArCH$_2$Ar), 123.5, 127.9, 130.2, 163.9 ppm (aromatic carbons). IR (KBr): ν = 2961vs, 2904s, 2866s, 2342w, 1601m, 1479vs, 1392s, 1317s, 1297vs, 1235m, 1200s, 1127s, 882 cm^{-1} (m). UV–Vis (THF) λ_{max}/nm (ε/dm^3 mol^{-1} cm^{-1}): 290 (4.191×10^4), 261 (3.844×10^4). Elemental Anal. Calc. for $C_{55}H_{67}O_5K_5 \cdot (C_4H_8O_3) \cdot CH_2Cl_2$: C, 62.69; H, 7.04. Found: C, 62.73; H, 7.28%.

5.6. Solubility and air-sensitivity of calixanions

All calixarene salts are very soluble in $CHCl_3$ and DMSO but less soluble in benzene or toluene. Most of the mono-, di- and trianionic salts are air stable, so it is easy to purify them by recrystallization. Their crystals readily lose solvent molecules to become powder. The salts **Bu^{t}C5** · Na and **Bu^{t}C5** · K were initially obtained as white powders. When they were left for one month in air they become green-brown and the ^{1}H NMR showed a significant increase in the amount of parent **Bu^{t}C5**. Most of the crystallizations were done in air, except for the air-sensitive pentaanions; their manipulation was performed under inert atmosphere.

5.7. VT-NMR studies

Temperature-dependent ^{1}H NMR spectra were recorded in a Varian XL-300 spectrometer at 300 MHZ, and the coolant was liquid nitrogen. The rate constants (k_c in s^{-1}) for conformational interconversion at the coalescence temperature were calculated from the equation $k_c = 2.22(\Delta\nu^2 + 6J_{AB}^2)^{1/2}$ [39,48–50]. The free energy barrier to conformational interconversion in kcal mol^{-1} was calculated from the equation $\Delta G^{\mp} = 4.58T_c(10.32 + \log T_c/k_c)/1000$. As in previous work, we assume an accuracy of ±5 °C for the value of T_c, an accuracy of ±15 Hz for the value of $\Delta\nu$, and an accuracy of ±2 Hz for the value of J_{AB}, and estimate that the values should be accurate to ±0.4 kcal mol^{-1} [39,48,49]. The value of $\Delta\nu$ was taken as the difference in Hz between the frequencies of the methylene doublets undergoing coalescence (observed at a sufficiently low temperature that the peaks are sharp) [39,48–50].

5.8. General X-ray crystal structure information

All crystal samples were colorless. X-ray data for **Bu^{t}C5** · Na_3 and **Bu^{t}C5** · K_2 were collected on a Bruker SMART APEX CCD diffractometer while all other data were collected on a Bruker SMART 1000 CCD detector. Both diffractometers used variable low temperature and Mo Kα radiation, and SADABS absorption corrections were applied. The crystals used in the experiments were coated with mineral oil, and data were collected under a variable low temperature nitrogen stream. Crystallographic data are summarized in Table 3. All structures were solved by direct methods and subsequent difference Fourier syntheses and refined by full matrix least-squares methods against F^2 (SHELX 97) [51]. Most solvent molecules as well as some *tert*-butyl groups are positionally disordered. All non-hydrogen atoms were refined anisotropically except for atoms of disordered fragments which were refined with isotropic thermal parameters. H atoms were constrained with a riding model. In the crystal structures of **Bu^{t}C5** · Na, **Bu^{t}C5** · Rb_2 and **Bu^{t}C5** · Na_3 · THF, disordered solvent molecules (6 THF molecules in **Bu^{t}C5** · Rb_2 and **Bu^{t}C5** · Rb_2, 7 THF molecules in **Bu^{t}C5** · Na_3 and one pentane molecule in **Bu^{t}C5** · Na) were treated with the program SQUEEZE [52]. Corrections of the X-ray data for **Bu^{t}C5** · Rb_2, **Bu^{t}C5** · Cs_2 **Bu^{t}C5** · Na_3 and **Bu^{t}C5** · Na by SQUEEZE (256, 239, 290 and 54 electron cell, respectively), were close to the required values (240, 240, 280 and 42 electron cell, respectively), similar to the results described previously [20]. The programs ORTEP32 [53] and POV-RAY [54] were used to generate the X-ray structural diagrams pictured in this article.

Acknowledgements

We are grateful to the Welch Foundation grant P-1459 and the National Science Foundation (Grant No. CHE-133866) for research funding. We are also grateful to Prof. Michael Lattman at Southern Methodist University for the loan of facilities and expertise for calix[5]arene syntheses.

Appendix A. Supplementary material

CCDC 681934, 681935, 681936, 681937, 681938, 681939, 681940, 681941, 681942, 681943, 681944 and 681945 contain the supplementary crystallographic data. These data can be obtained free of charge from The Cambridge Crystallographic Data Centre via www.ccdc.cam.ac.uk/data_request/cif. Supplementary data associated with this article can be found, in the online version, at doi:10.1016/j.jorganchem.2008.12.065.

References

[1] C.D. Gutsche, Calixarenes, Royal Society of Chemistry, Cambridge, 1989.
[2] W. Sliwa, J. Inclus. Phenom. Macrocyc. Chem. 44 (2005) 13–37.
[3] U. Radius, Z. Anorg. Allg. Chem. 630 (2004) 957–972.
[4] C. Redshaw, Coord. Chem. Rev. 244 (2003) 45–70.
[5] C. Floriani, R. Floriani-Moro, Adv. Organomet. Chem. 47 (2001) 167–233.
[6] C. Wieser, C.B. Dieleman, D. Matt, Coord. Chem. Rev. 165 (1997) 93–161.
[7] C.D. Gutsche, Calixarenes Revisited, Royal Society of Chemistry, Cambridge, 1998.
[8] A. Zanotti-Gerosa, E. Solari, L. Giannini, C. Floriani, A. Chiesi-Villa, C. Rizzoli, Chem. Commun. (1997) 183–184.
[9] R. Arnecke, V. Böhmer, R. Caccipaglia, A.D. Cort, L. Mandollini, Tetrahedron 53 (1997) 4901–4908.
[10] T. Haino, M. Yanase, Y. Fukazawa, Angew. Chem., Int. Ed. Engl. 36 (1997) 259–260.
[11] V. Bohmer, Angew. Chem., Int. Ed. Engl. 34 (1995) 713–745.
[12] Z. Asfari, V. Böhmer, J. Harrowfield, J. Vicens, Calixarenes, Kluwer Academic Publishers, Dordrecht, 2001.
[13] P.D. Harvey, Coord. Chem. Rev. 233–234 (2002) 289–309.
[14] S.E.J. Bell, J.K. Browne, V. McKee, M.A. McKervey, J.F. Malone, M. ÓLeary, A. Walker, J. Org. Chem. 63 (1998) 489–501.
[15] C. Floriani, Chem. Eur. J. 5 (1999) 19–23.
[16] A.W. Coleman, S.G. Bott, S.D. Morley, C.M. Means, K.D. Robinson, H. Zhang, J.L. Atwood, Angew. Chem., Int. Ed. Engl. 27 (1988) 1361–1362.
[17] R.M. Izatt, J.D. Lamb, R.T. Hawkins, P.R. Brown, S.R. Izatt, J.J. Christensen, J. Am. Chem. Soc. 105 (1983) 1782–1785.
[18] F.P. Ballistreri, A. Notti, S. Pappalardo, M.F. Parisi, I. Pisagatti, Org. Lett. 5 (2003) 1071–1074.
[19] D. Garozzo, G. Gattuso, F.H. Kohnke, A. Notti, S. Pappalardo, M.F. Parisi, I. Pisagatti, A.J.P. White, D.J. Williams, Org. Lett. 5 (2003) 4025–4028.
[20] T.A. Hanna, L. Liu, A. Angeles-Boza, X. Kou, C.D. Gutsche, K. Ejsmont, W.H. Watson, L.N. Zakharov, C.D. Incarvito, A.L. Rheingold, J. Am. Chem. Soc. 125 (2003) 6228–6238.
[21] T.A. Hanna, L. Liu, L.N. Zakharov, A.L. Rheingold, W.H. Watson, C.D. Gutsche, Tetrahedron 58 (2002) 9751–9757.
[22] U.C. Meier, C. Detellier, Supramol. Chem. 9 (1998) 289–295.
[23] F.T. Ladipo, V. Sarveswaran, J.V. Kingston, R.A. Huyck, S.Y. Bylikin, S.D. Carr, R. Watts, S. Parkin, J. Organomet. Chem. 689 (2004) 502–514.
[24] L. Salmon, P. Thuéry, M. Ephritikhine, Dalton Trans. 30 (2006) 3629–3637.
[25] P. Sood, M. Koutha, M. Fan, Y. Klichko, H. Zhang, M. Lattman, Inorg. Chem. 43 (2004) 2975–2980.
[26] M. Fan, H. Zhang, M. Lattman, Chem. Commun. (1998) 99–100.
[27] M. Fan, H. Zhang, M. Lattman, Inorg. Chem. 45 (2006) 6490–6496.
[28] L. Salmon, P. Thuéry, M. Ephritikhine, Eur. J. Inorg. Chem. (2006) 4289–4293.
[29] F. Hamada, K.D. Robinson, G.W. Orr, J.L. Atwood, Supramol. Chem. 2 (1993) 19–24.
[30] J.M. Harrowfield, M.I. Ogden, W.R. Richmond, A.H. White, Chem. Commun. (1991) 1159–1161.
[31] P. Thuèry, Z. Asfari, J. Vicens, V. Lamare, J.-F. Dozol, Polyhedron 21 (2002) 2497–2503.

[32] E.D. Gueneau, K.M. Fromm, H. Goesmann, Chem. Eur. J. 9 (2003) 509–514.
[33] L. Liu, L.N. Zakharov, A.L. Rheingold, T.A. Hanna, Chem. Commun. (2004) 1472–1473.
[34] L. Liu, L.N. Zakharov, J.A. Golen, A.L. Rheingold, W.H. Watson, T.A. Hanna, Inorg. Chem. 45 (2006) 4247–4260.
[35] L.J. Charbonnière, C. Balsiger, K.J. Schenk, J.-C.G. Bünzli, J. Chem. Soc., Dalton Trans. (1998) 505–510.
[36] D.R. Stewart, M. Krawiec, R.P. Kashyap, W.H. Watson, C.D. Gutsche, J. Am. Chem. Soc. 117 (1995) 586–601.
[37] F. Arnaud-Neu, Z. Asfari, B. Souley, J. Vicens, P. Thuéry, M. Nierlich, J. Chem. Soc., Perkin Trans. 2 (2000) 495–499.
[38] A.J. Petrella, N.K. Roberts, D.C. Craig, C.L. Raston, R.N. Lamb, Chem. Commun. (2003) 1728–1729.
[39] D.R. Stewart, C.D. Gutsche, J. Am. Chem. Soc. 121 (1999) 4136–4146.
[40] K. Murayama, K. Aoki, Inorg. Chim. Acta 281 (1998) 36–42.
[41] T.J. Boyle, D.M. Pedrotty, T.M. Alam, S.C. Vick, M.A. Rodriguez, Inorg. Chem. 39 (2000) 5133–5146.
[42] D.C. Bradley, R.C. Mehrotra, I.P. Rothwell, A. Singh, Alkoxo and Aryloxo Derviatives of Metals, Academic Press, New York, 2001.
[43] B.W.F. Gordon, M.J. Scott, Inorg. Chim. Acta 297 (2000) 206–216.
[44] M.G. Davidson, J.A.K. Howard, S. Lamb, C.W. Lehmann, Chem. Commun. (1997) 1607–1608.
[45] G. Guillemot, E. Solari, C. Rizzoli, C. Floriani, Chem. Eur. J. 8 (2002) 2072–2080.
[46] J.W. Steed, C.P. Jhonson, C.L. Barnes, R.K. Juneja, J.L. Atwood, S. Reilly, R.L. Hollis, P.H. Smith, D.L. Clark, J. Am. Chem. Soc. 117 (1995) 11426–11433.
[47] D.R. Stewart, C.D. Gutsche, Org. Prep. Proc. Int. 25 (1993) 137–139.
[48] C.D. Gutsche, L.J. Bauer, J. Am. Chem. Soc. 107 (1985) 6059–6063.
[49] S. Kanamathareddy, C.D. Gutsche, J. Org. Chem. 59 (1994) 3871–3879.
[50] H. Friebolin, Basic One- and Two-Dimensional NMR Spectroscopy, Wiley-VCH, Weinheim, 1998. pp. 307–312.
[51] G.M. Sheldrick, SHELX97, Program for Crystal Structure Solution and Refinement, University of Göttingen, Göttingen, Germany, 1998.
[52] P.V. van der Sluis, A.L. Speck, Acta Crystallogr. A 46 (1990) 194–201.
[53] L.J. Farrugia, J. Appl. Cryst. 30 (1997) 565.
[54] Persistence of Vision Raytracer, Persistence of Vision Pty. Ltd., Williamston, Victoria, Australia, 2002, Retrieved from <http://www.povray.org/download/>.